Metal–organic frameworks and their derived materials in water purification

Please, cite as follows:

Chizoba I. Ezugwu, Srabanti Ghosh, Marta E.G. Mosquera, Roberto Rosal. Metal-organic frameworks and their derived materials in water purification, Chapter 12 in Srabanti Ghosh, Aziz Habibi-Yangjeh, Swati Sharma y Ashok Kumar-Nadda (Eds.) Nanomaterials for Water Treatment and Remediation, CRC Press, 1st Ed., 2021, eBook ISBN9781003118749, https://doi.org/10.1201/9781003118749

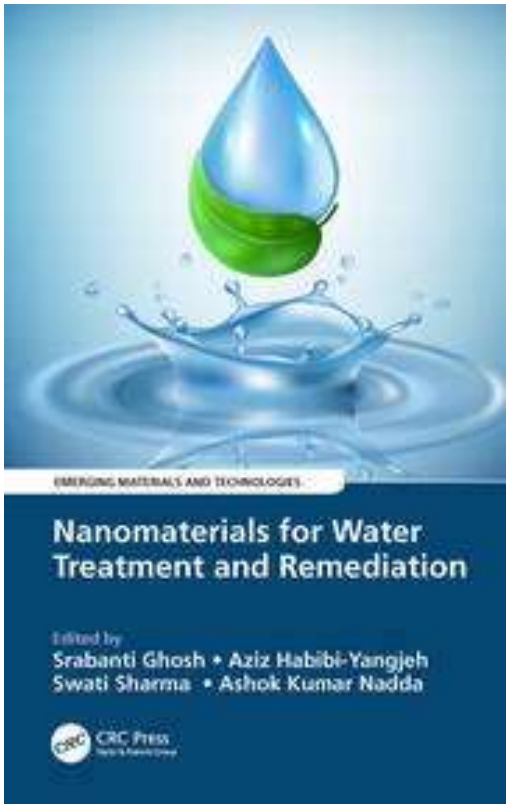

Metal–organic frameworks and their derived materials in water purification

Chizoba I. Ezugwu[1,*], Srabanti Ghosh[2], Marta E.G.Mosquera[2], Roberto Rosal[1]

1 Department of Analytical Chemistry, Physical Chemistry and Chemical Engineering, University of Alcalá, Alcalá de Henares, E-28871 Madrid, Spain

2 Department of Organic and Inorganic Chemistry, Instituto de Investigación en Química "Andrés M. del Río" (IQAR), Universidad de Alcalá, Campus Universitario, 28805, Alcalá de Henares, Madrid, Spain

[*] Corresponding author: chizoba.ezugwu@uah.es

Abstract

Water pollution is a global problem that affects sustainable development. Metal–organic frameworks (MOFs) have recently attracted great attention in water purification due to their high crystallinity, exceptional large surface area, ultra-high porosity, availability of accessible active sites, surface functionality, and accessible structural tunability. The present chapter highlights the recent advances in the use of MOFs and their derivatives for the efficient removal of contaminants in wastewater. In particular, photocatalysis, sulfate radical-based advanced oxidation process (SR-AOPs), heavy metals and organic pollutants removal, and MOFs-mixed matrix membranes (MOF-MMMs) strategies are detailed in the discussion. This chapter further provides an overview on the synthesis, components, and secondary building units of MOFs together with MOF-derived materials. The mechanisms of the interaction between these frameworks and the contaminants are also summarized.

Keywords: Metal–organic frameworks; Water treatment; Contaminants; Separation strategies; Interaction mechanisms

1. Introduction

One of the most critical global environmental challenges threatening humanity is water pollution caused by the rapid growth in industrialization and other anthropogenic activities. The incessant release of chemicals due to agricultural production (pesticides, fungicides, herbicides, and insecticides) and industrial waste like organic (dyes) and inorganic pollutants (heavy metals) that are wastewater contaminants, constitutes serious environmental concern (Bedia et al., 2019). In addition, emerging organic contaminants comprising pharmaceuticals, detergents, personal care products, caffeine, steroids, and hormones, plasticizers, and flame retardants, among others, have been identified in wastewater in concentrations usually ranging from ppt to ppb (Rodriguez-Narvaez et al., 2017). The risk of emerging pollutants for human health and the entire biodiversity has been highlighted elsewhere (Taheran et al., 2018; Rout et al., 2020). Furthermore, the continuous increase in the world population results in an exponential rise for clean drinking water demand. Although 72 % of the Earth's surface is occupied by water, only 0.5 % is freshwater (Jun et al., 2020). Moreover, most water-intensive activities such as energy production and agriculture are anticipated to increase the global water demand from 60% to 85% over the next three decades (Boretti & Rosa, 2019). Global warming is another factor impacting the availability of water resources. This stresses that water resources are becoming seriously scarce and that there is an urgent need to address this global problem to avoid potential conflicts among water users (Tzanakakis et al., 2020).

Until now, researchers have prepared various materials for wastewater purification (Siegert et al., 2019). For example, zeolites, activated carbon, magnetic materials, chitosan, graphene, and metal oxides have been widely described (Mário et al., 2020). Notwithstanding that most of them have been successfully used for wastewater treatment, there is still a need to enhance their performance (Lee et al., 2012). The increased demand for efficient materials together with the need for purified water, induced the development of advanced hybrid nanomaterials, notably those based on metal–organic frameworks (MOFs). Recently, there have been a tremendous improvement in this class of porous coordination polymers (Mukherjee et al., 2018). Their pores and linkers can be easily functionalized, which is advantageous when compared to conventional inorganic and organic microporous materials (Li et al., 1999). The basic idea for the design and preparation of MOFs is derived from metal carboxylate cluster chemistry, i.e., through the interface between coordination chemistry and material sciences (Yang et al., 2020). Metal–organic frameworks were first reported by the research groups of (O.M. Yaghi et al., 1995) and S. Kitagawa (Kondo et al., 1997). The main feature of these framework materials is that their crystal structures are retained after evacuation of solvent, which can be proven by X-ray single-crystal analyses (Figure 1). Extensive research attention has been directed toward the synthesis of new MOFs and their applications due to their promising properties

https://doi.org/10.1201/9781003118749

(Smolders et al., 2018; Joharian & Morsali, 2019; Mason et al., 2014). For industrial applications, the main challenge of MOFs is their stability as the coordination bonds between the ligand and metal components are weak, hence their thermal and chemical stability are generally lower when compared to zeolites. Also, some MOFs are moisture- and air-sensitive following evacuation of the pores and should be handled under inert atmosphere.

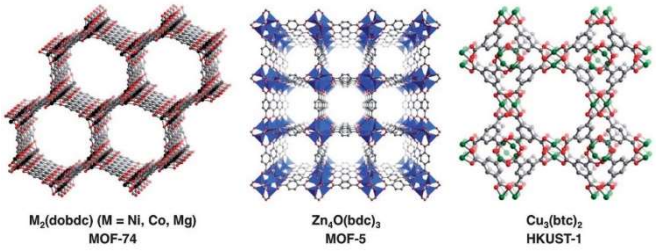

Figure 1. Crystal structures of some representative MOFs. Reproduced with Permission from Chem. Sci., 2014, 5, 32–51.

MOFs materials possess significantly high surface areas along with the lowest densities per gram when compared to competing materials (Furukawa et al., 2010; Farha et al., 2012). These distinctive features make them suitable for environmental applications, like the removal of pollutants by adsorption, which have been extensively investigated (Wang et al., 2016; Khan & Jhung, 2017; Ezugwu et al., 2018, 2019). Their shape, pore size, and functionality played an essential role in the selective adsorption of pollutants from contaminated water. The fundamental adsorption mechanisms include acid-base π-π interactions/stacking, electrostatic, hydrophobic, and hydrogen bonding (Hasan & Jhung, 2015). MOFs have proven to be good adsorbents for water contaminated with industrial and agricultural wastes such as dyes, pesticides, herbicides, pharmaceuticals, and personal care products (PPCP) (Haldar et al., 2020; Hasan et al., 2020), and heavy metals (Dias & Petit, 2015; Shayegan et al., 2020). Sulfate radical-based advanced oxidation process (SR-AOPs), photocatalysis, MOFs-mixed matrix membranes (MMMs) and ion exchange are other techniques for treating wastewater using MOFs.

2. Components of MOFs and secondary building units (SBUs)

2.1. Components

MOFs are composed of metal-based nodes coordinated with organic ligands, resulting from 1D to 3D coordination networks (Ezugwu et al., 2016; Langmi et al., 2016). They are sometimes termed hybrid organic-inorganic materials. However, this has been disallowed by the IUPAC (Batten et al., 2013). The possibility of changing these components (linking unit and metal ion) makes it possible to construct a wide range of metal–organic frameworks. The organic linkers used for MOFs syntheses are from mono- to tetravalent ligands, which can donate electron lone pairs to the metal ions that contain vacant orbitals able to accept them. The choice of the ligand and metal ion together with their rational combination determines the structure and properties of the MOFs. For example, the affinity of the metal ion to bind to a particular ligand affects the pore size and influences the number of ligands that can coordinate to the metal. Normally, the two groups of ligands that are commonly employed for the preparation of MOFs are nitrogen-and oxygen-donor ligands, dominated by pyridyl- and carboxylate-containing linkers, respectively (Cook et al., 2013).

Figure 2 shows some N-donor ligands. For these ligands, the nitrogen atom makes use of its lone electron pair to coordinate to the metal ions (Zhang et al., 2018). To build MOFs with a particular topology, the functionality, shape, and size of the ligand can be rationally selected. Thus, ditopic ligands (i.e., ligands able to coordinate at two different sites) with an angle of 180°, like 4,4′-bpy, may form molecular frameworks with varied dimensionality. The final structure of MOFs constructed from these ligands is usually pre-determined by the metal node (Jin et al., 2019). The main limitation of using N-donating ligands for MOFs synthesis is the easy decomposition of the extended structure due to the weak coordination bonds.

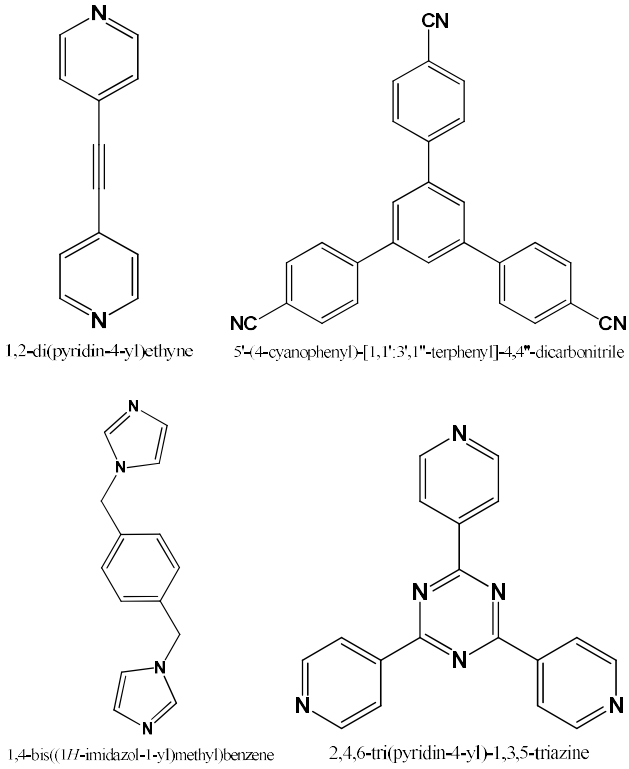

Figure 2. N-donor ligands employed for the preparation of MOFs.

Carboxylate compounds are the most frequently used O-donor ligands. They have stronger chelation capacity than N-donating ligands and are the most common choice for MOF synthesis. The negatively charged carboxylate ligand neutralizes most of the positively

https://doi.org/10.1201/9781003118749

charged metal ions in the MOFs. Importantly, this may reduce the number of counter-anions needed, which could otherwise occupy part of the available space within the internal cavities and channels (Zhao et al., 2019). As shown in Scheme 1, carboxylates can display three different binding modes: monodentate, bidentate chelate, and bidentate-bridging. The versatility offered by different binding modes (chelate and bridging) and their stronger coordination bonds make carboxylate-based ligands (Figure 3) are more suitable for MOFs synthesis.

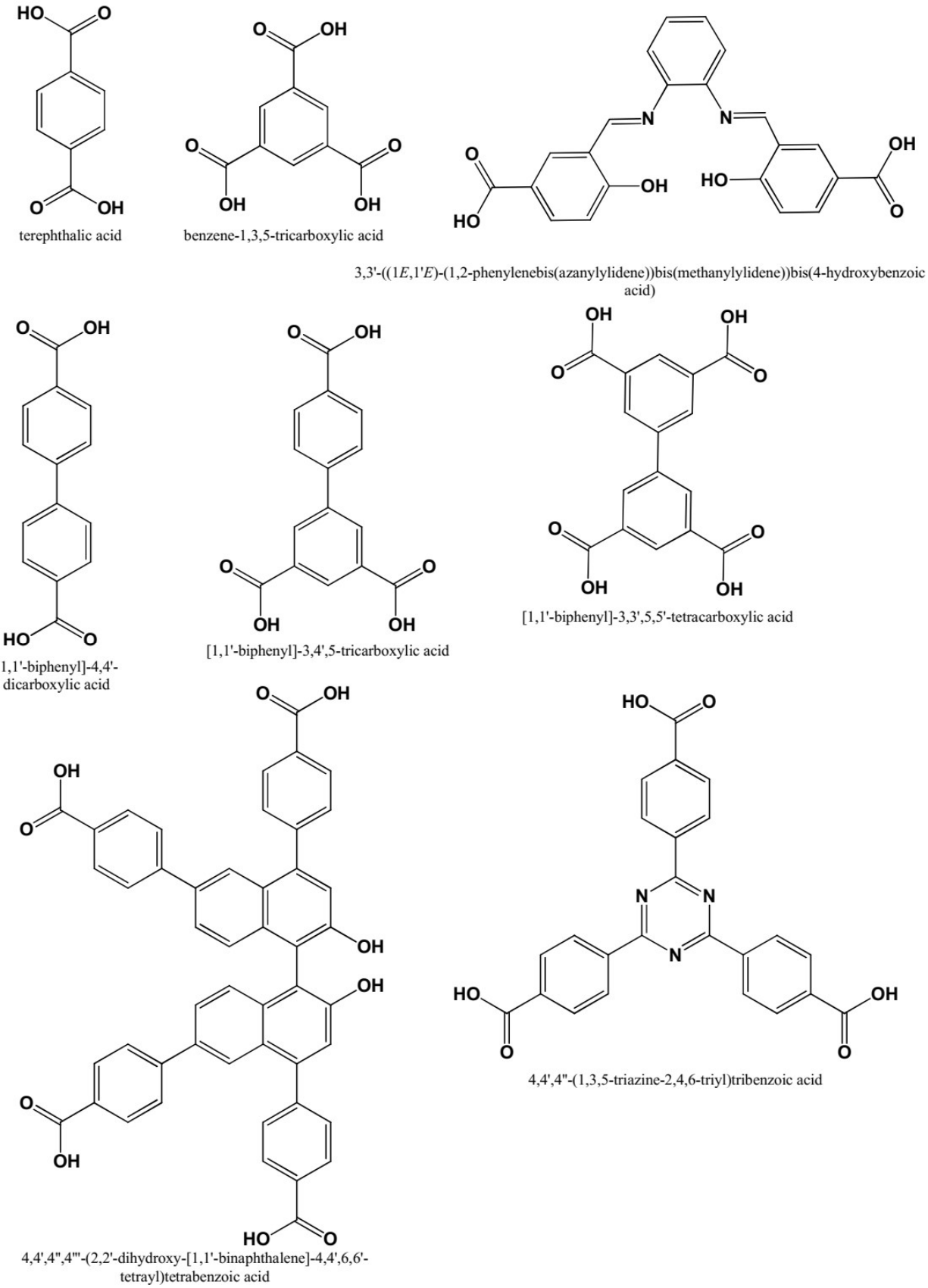

Figure 3. Some carboxylate-based ligands used for MOFs synthesis.

https://doi.org/10.1201/9781003118749

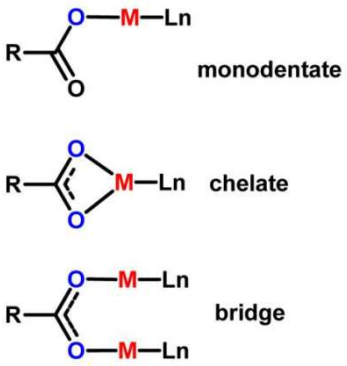

Scheme 1. Binding modes of carboxylate linkers. Permission taken from Chem. Rev., 2013, 113, 734–777.

2.2. Secondary building units

In MOF formation, the major restriction for using a single metal ion is the limitations of orientations, which results in low-quality frameworks with high defective sites. Yaghi et al. (2003) developed a versatile and fruitful design strategy, termed reticular chemistry. This approach utilizes secondary building units (SBUs) as molecular polygons for MOFs formation (Guillerm & Maspoch, 2019; Gropp et al., 2020). These SBUs are well-defined metal clusters rigid in nature, so they maintain their directionality during the self-assembly process (Tranchemontagne et al., 2009). Some common SBUs employed in MOFs synthesis are presented in Figure 4. These are unit of "polynuclear clusters" designed from multidentate ligands and two/more metal ions. The organic ligand extends out from these SBU's in an ordered geometry to forms the MOFs structure. Notably, when the geometry and site of SBUs are considered, the network topology can be predicted.

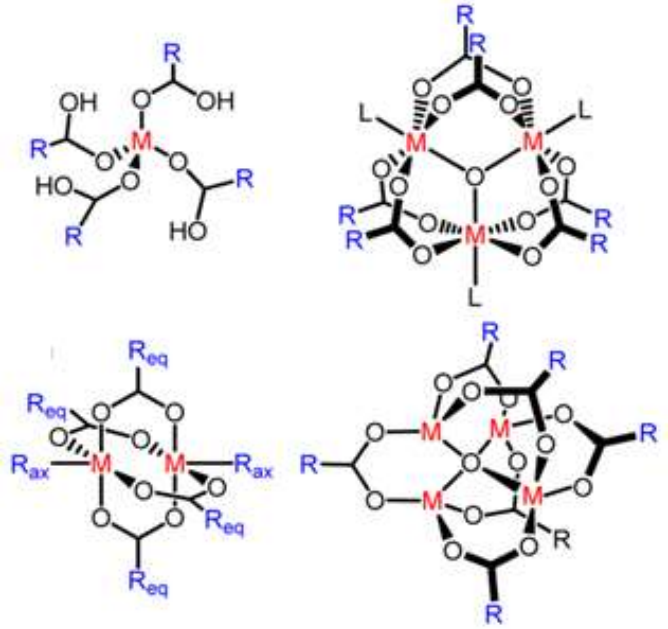

Figure 4. Structural illustration of some common SBUs. Permission taken from Chem. Rev., 2013, 113, 734–777.

SBUs are not reagents in a synthetic scheme, but they are in-situ generated during MOFs synthesis and depend on the reaction conditions and precursors (Rowsell & Yaghi, 2004). The introduction of SBUs helps to comprehend the geometry formed around the metal nodes of the frameworks. In terms of design and utility, the development of these units increases the cavity and pores of the MOFs, as well as allowing higher surface area. The SBUs can control the different coordination modes of transition metals during the synthesis of the material. Generally, transition metal ions are mainly employed as the metal nodes of the SBUs owing to their inherent properties of adopting varied coordination numbers, which results in different geometry (Kalmutzki et al., 2018). Metals from the first row are commonly used due to their low cost, availability, and thorough understanding of their chemistry.

3. Synthesis of metal–organic frameworks

The rationale for using different synthetic methods to prepare MOFs is the need to take advantage of all the possible frameworks that can be obtained using different synthesis approaches (Stock & Biswas, 2012). Alternative synthetic methods can produce frameworks with different morphologies and particle size, thereby influencing the overall properties of the material. The particle sizes of MOFs have a direct influence on the diffusion rate/capacity of guest molecules, thus affecting the adsorption and separation efficiencies of the material.

Basically, MOFs are prepared by mixing organic ligand and metal salt in a vessel (Figure 5) followed by providing the required condition for their formation (Abednatanzi et al., 2019). The two common techniques adopted for the preparation of MOFs can be classified into the conventional and unconventional methods.

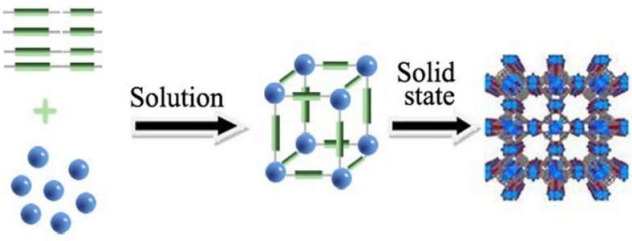

Figure .5. Metal ions combination with the ligands to synthesize MOFs materials. Reproduced with permission from Coord. Chem. Rev., 2016, 307, 188–210.

i. Conventional synthesis

This synthetic method is usually applicable to reactions achieved by conventional heating without side reactions. One of the key parameters considered in this synthesis is the reaction temperature. Conventional syntheses can follow either solvothermal or non-solvothermal route. Solvothermal synthesis simply involves heating the reactants in closed vessels (normally Teflon-lined autoclave) under pressure and above the solvent's boiling point, which usually contain formamide functionality, like dimethylformamide

https://doi.org/10.1201/9781003118749

(DMF) and N, N-diethylformamide (DEF) (Safaei et al., 2019). Some prominent MOFs/MOFs composite, applied for the treatment of contaminated water, have been obtained by these methods (Joseph et al., 2019; Sule & Mishra, 2019; Olawale et al., 2020). Crystalline MOFs with high surface area prepared by this approach are often suitable for X-ray crystallography. Good crystallization is achieved by optimizing the amount of solvent and reaction temperature (Vardhan et al., 2016). Nevertheless, the limitations of solvothermal synthesis include high energy requirements, long reaction time, and nitrogen-containing organic solvents, which are not always environmentally benign. Furthermore, some frameworks prepared by this method are thermally unstable or even can react with the solvent.

ii. Unconventional synthetic method

The methods for preparing MOFs without using conventional heating are termed unconventional synthesis. They include electrochemical, microwave-assisted, mechanochemical, sonochemical, and solvent-free synthesis techniques. The main objective of these methods is the absence of anions like nitrate and chloride during the synthesis. In the electrochemical method, the metal ions are produced from the metal electrode (Cao et al., 2019; Wei et al., 2019), whereas in the mechanochemical method, a mechanical force is applied to the reactant mixture containing the solid reactant and little solvent (Chen et al., 2019). Unlike solvothermal synthesis that takes a long reaction time (days sometimes), the reaction time is reduced to reach even seconds for microwave-assisted synthesis. The reactants are activated by microwave irradiation (Chang et al., 2019b). However, the limitation with the microwave method is the rapid nucleation and crystal growth, which results in a higher amount of crystal defects and low internal surface area (Mousavi et al., 2018). MOFs can also be prepared by ionothermal techniques that use ionic liquids, fulfilling a dual role as the solvent and templating agent, thereby minimizing the number of species involved in the synthesis (Luo et al., 2019).

4. MOF-derived materials

MOFs have been used as a template for the preparation of different nanostructured materials, like transition metal oxides, heteroatom-doped carbons, and carbon materials by calcination and pyrolysis under appropriate conditions. For example, nanoporous metal/carbons composites can be generated by the pyrolysis of a MOF precursor under an inert atmosphere. Furthermore, direct heat treatment of the framework can form porous metal oxides (Salunkhe et al., 2017), and carbon materials can be produced by etching off the residual metal (Liu et al., 2018a). Some of the advantages of these MOF-derived materials include higher stability, enhanced performance, expanded surface area/porosity and facile synthesis (Jiang et al., 2019).

i. Carbonization

The stability of MOF materials can be improved by introducing functional groups or direct carbonization of MOF-derived materials. Porous carbons prepared from a metal azolate framework-6 (MAF-6) via different pyrolysis times were used to remove artificial sweeteners (acesulfame, saccharin, and cyclamate) from water (Song et al., 2018). Interestingly, these porous carbons have surface functionality, high porosity, stability, and hydrophobicity. The pyrolysis temperature and time influenced the adsorption process. The samples prepared for 6 h exhibited higher saccharin adsorption (93 mg/g) from the water after 12 h, compared to activated carbon (4.7 mg/g). The main interaction mechanism was assigned to H-bonding; the surface functional phenolic group in the porous carbon acts as the H-donor, while artificial sweeteners act as the H-acceptor.

Liu et al. (2018b) used a fast and facile method of short-term high-temperature approach for the preparation of a functional carbon material (TEPA-C-MOF-5), which was derived from MOF-5. During the synthesis, tetraethylenepentamine (TEPA) doped MOF-5 materials were carbonized at 500 °C for several seconds under an air atmosphere, the sample changed from white to dark yellow, Scheme 12.2. The prepared carbonized material demonstrated a higher adsorption of U (VI) than the parent MOF-5, 550 mg/g at a relatively low pH (3.5).

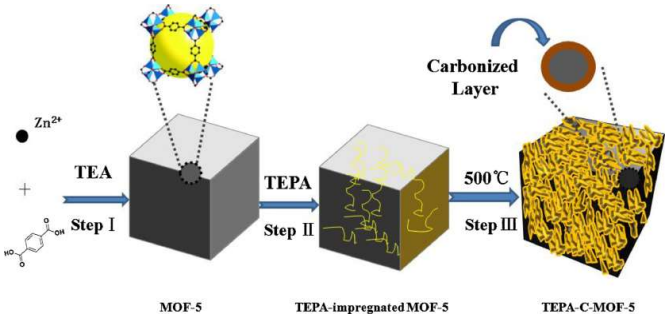

Scheme 2. The formation process of the carbonized sorbent. Permission taken from Colloids Surf. A Physicochem. Eng. Asp., 2018, 556, 72–80.

Incorporating heteroatoms, such as N, O, and S, into a porous carbon material can be used to enhance their interaction with substrates. Xu et al. (2017) employed ZIF-8 as a self-sacrificial template to synthesize nitrogen-doped porous carbons by first forming ZIF/dicyandiamide (Carbon-ZD) and ZIF/sucrose (Carbon-ZS) composites, followed by carbonization at 950°C under argon atmosphere. Using excess Carbon-ZD to treat wastewater proved an excellent candidate for methylene blue (MB) removal with almost 100% efficiency.

ii. Deposition of Metal Nanoparticles

https://doi.org/10.1201/9781003118749

A high number of magnetic Co nanoparticles uniformly dispersed on nanoporous carbon particles (Co/NPC) were successfully prepared via one-step carbonization of ZIF-67 (Torad et al., 2014). The graphitic carbon has a strong affinity to aromatic compounds, while the zeolite-like pore structure is good for adsorbing metal ions. The obtained composite showed a well-developed graphitized wall with high surface area, thereby exhibiting fast diffusion and excellent adsorption capacity (500 $mg \cdot g^{-1}$) of MB. Interestingly, 99.9 % of the MB was captured into Co/NPC sample after 24 h. Compared with the commercial activated carbon, Co/NPC particles showed impressive saturation capacity for MB dye.

Ahsan et al. (2019) prepared Ni and Cu nanoparticles-embedded carbon sheets (C@Ni and C@Cu) via annealing of Cu-BDC and Ni-BDC MOFs, at 600°C under an inert environment. SEM and TEM analyses illustrated the deposition of the metallic Cu and Ni particles on the nanoporous carbon sheet. The developed nano-catalysts were investigated for the NaBH4-mediated reduction of 4-nitrophenol, methyl orange (MO), and MB. They showed efficient nature for the degradation of these water pollutants to their corresponding reduced organic molecules in about 60 s.

iii. Heterostructured MOFs-Derived Semiconductor Composites

Cobalt-containing magnetic carbonaceous nanocomposite (MCN) was prepared from the carbonization of cobalt-based MOF, ZIF-67 at 600 °C under N_2 atmosphere (Lin et al., 2015a). The Co_3O_4/C (MCN) composite showed catalytic activity for Oxone (a triple salt of potassium peroxymonosulfate) activation to degrade rhodamine B(RhB) in water. Efficient activation process was observed at Oxone/MCN ratio of 5/1. The heterogenous catalyst has high saturation magnetization (45 emu g^{-1}), allowing their separation from water to be easy (Lin et al., 2015a). Gong et al. (2018) fabricated heterostructured ZIF-NC/g-C_3N_4 composite, which manifested enhanced decomposition of bisphenol A under light, displaying an apparent rate constant with peroxymonosulfate (PMS) and outperforming g-C_3N_4 with a value 8.4 times higher. The improved activity was attributed to the efficient interfacial charge separation between ZIF-NC and g-C_3N_4 together with the abundant surface-active sites for the activation of PMS to $SO4^{\bullet-}$.

Li et al. (2020) prepared a lotus leaf-like aerogel composed of MOF nanocoating and kapok fiber (a cellulosic fiber from the kapok tree) core. The aerogel was synthesized by growing hydrophobic zeolitic imidazolate frameworks-8 (ZIF-8) on the surface of kapok, which was triggered by Fe^{3+}-tannic acid networks (FTN, a kind of metal-phenolic network). The as-prepared ZIF-8FTN/kapok aerogel showed an ultrahydrophobic surface with a water contact angle of up to 162 °C. In addition, this composite has the capacity to adsorb oil/organic (20.0–72.0 g $(sorbent)^{-1}$), 17–40 times higher compared to ZIF-8. The superior capacity was attributed to the ZIF-8 being supported to the kapok aerogel.

5. Strategies for using MOFs in wastewater treatment

5.1. Sulfate radical-based advanced oxidation processes

Advanced oxidation processes (AOP) constitute a family of innovative wastewater treatment technologies based on the production of highly reactive radicals, like superoxide ($O2^{\bullet-}$), hydroperoxyl radical ($OOH^{\bullet}$), hydroxyl radical ($OH^{\bullet}$), and sulfate radical ($SO_4^{\bullet-}$) (Chen et al., 2019; Milenković et al., 2020; Zhao et al., 2020). Sulfate radical-based advanced oxidation process (SR-AOPs) is characterized by the in-situ production of sulfate radicals from certain salts and gained popularity in wastewater treatment due to its high selectivity even in complex matrices. $SO_4^{\bullet-}$ is a strong oxidant capable of degrading many organic pollutants. The three main reaction mechanisms of $SO_4^{\bullet-}$ with organic pollutants are: (a) abstraction of hydrogen atom from esters, ethers, alcohol and alkanes; (b) single-electron transfer from compounds with electron-donating groups like amines and hydroxyl moieties; and (c) the addition reaction of $SO_4^{\bullet-}$ to organic compounds that contain unsaturated bonds (Luo et al., 2017; Xiao et al., 2018; George et al., 2001).

It has been reported that SR-AOPs overperform the traditional •OH-based AOPs; $SO_4^{\bullet-}$ can work over a wider pH range during the degradation of organic pollutants. It displays higher efficiency to degrade pollutants containing unsaturated bonds/aromatic ring and has higher oxidation potential (2.6–3.1 V for $SO_4^{\bullet-}$ versus 2.8 V for $HO^{\bullet}$) (Wang et al., 2019). Moreover, the sulfate radical has a longer half-life (30–40 µs) and better selectivity when compared to its hydroxyl radical counterpart (Ahmed et al., 2012; Zhu et al., 2019)

Heterogenous catalysts are employed to form $SO_4^{\bullet-}$ by the activation (either physically or chemically) of persulfate (PS, $S_2O_8^{2-}$) or peroxymonosulfate (PMS, HSO_5^-). The activation by ultraviolet light, thermal, alkaline, metal oxides, metal-free materials, transition metal ions (Co^{2+}, Cu^{2+} and Fe^{2+}) and carbonaceous-based materials generate $SO_4^{\bullet-}$ (Ismail et al., 2017; Wang & Wang, 2018; Xiao et al., 2018). The O-O bond energy in PS is 140 kJ/mol and that of PMS is in the range of 140–213.3 kJ/mol. Therefore, the formation of sulfate radicals at least requires the minimum energy for O-O bond cleavage (Yang et al., 2010; Wang & Wang, 2018). The cleavage of O-O bond by heating can be achieved at a temperature >50 °C. It can also be activated by ultrasound; in this case, the activation mechanism involves the production of cavitation bubbles, which initiate the activation process (Neppolian et al., 2010). In alkaline conditions, the

activation requires a nucleophilic attack on the O-O bond, achieved by the addition of hydroxide (Furman et al., 2010).

Although iron and its oxides were the most investigated homogenous metals to activate PS and post-synthetic modification (PSM), cobalt ion proved best performance for activating PMS while PM was best activated with silver ion (Rastogi et al., 2009; Hu & Long, 2016). Compared to homogenous catalysts for PS/PMS activation, heterogeneous catalysts are a more efficient strategy owing to higher energy savings and convenient catalyst recovery. Although metal-based catalysts exhibit high efficiency for activating PMS or PS, attention must be paid to the possible leaching of potentially toxic metals out of the system. On the other hand, most carbon-based materials have insufficient activity (Hu et al., 2017). Therefore, the design of novel and more efficient catalysts for PS/PMS activation is of great technological interest.

MOFs have been successfully applied for PS/PMS activation owing to their inherent unique features. Both the metal clusters and the organic ligand of MOFs can be modulated to enhance their activation capacity. Their PS/PMS activation capacity can be enhanced by three major strategies: structural and morphological optimization; modification of the framework's metal-cluster and/or ligand via functionalization; and fabrication of MOF composites (Du & Zhou, 2020).

The degradation efficiency of MOF-based materials for organic dyes in SR-AOPs is related to particle size, structural topology, and cage size. Gao's group prepared ZIF-9 and ZIF-12 with the same composition of Co^{2+} and organic linker but having different structural topologies and particle size (Cong et al., 2017). The two MOFs were employed as PMS activation catalysts for RhB degradation. ZIF-9 had closer contact with PMS due to its nanoscale nature, allowing a higher degradation ratio (54.8 %) than ZIF-12 (27.7 %). Fe-based MILs such as MIL-100(Fe), MIL-101(Fe), MIL-88B(Fe), and MIL-53(Fe) were introduced as catalysts and adsorbents to generate sulfate radicals and hydroxyl radicals from PS for the degradation of acid orange 7(AO7) dye in water (Li et al., 2016). The adsorption and catalytic capacities of these materials were in the sequence MIL-101(Fe) > MIL-100(Fe) > MIL-53(Fe) > MIL-88B(Fe), which was directly related to the activity of the metal ion in catalyst sites and the different cage sizes. Furthermore, both hydroxyl radicals and sulfate radicals were the reactive species. As illustrated in Figure 6a, the mechanism for the catalytic degradation of AO7 by MIL-101(Fe)/PS starts by the PS diffusing into the open pore framework of MILs, which is favored by its big cage size. Then PS is activated by Fe (III) to yield $S_2O_8^{\bullet-}$ and Fe(II), after which Fe(II) is re-oxidized by PS to generate $SO_4^{\bullet-}$ (Li et al., 2016). Gao et al. (2017) further reported that the degradation of AO7 using MIL-53(Fe) under the irradiation of visible LED light was unsatisfactory due to the fast recombination of photoinduced electron-hole pairs, which was suppressed by the introduction of PS as an external electron acceptor. The addition of PS together with the formation of reactive $SO_4^{\bullet-}$ and $HO^{\bullet}$ radicals synergistically accelerated the light-induced degradation of AO7.

As aforementioned, integrating MOFs with other functional materials in order to form MOFs composites is a good strategy for preparing efficient catalysts for SR-AOPs. A yolk-shellCo_3O_4@MOFs nanoreactor was designed and used to incorporate SR-AOPs into its interior cavity (Zeng et al., 2015). The nanoreactor was applied as a catalyst for 4-chlorophenol (4-CP) degradation in the presence of PMS. The mesoporous MOFs shells promoted the fast diffusion of the reactants (4-CP and PMS) into the encapsulated active sites (Co_3O_4), and the confined high concentration of these reactant molecules in the local void space facilitated the SR-AOPs. The Co_3O_4@MOFs catalysts showed enhanced SR-AOPs with 4-CP degradation efficiency of almost 100 % within 60 min, whereas only 59.6 % was degraded for bare Co_3O_4 NPs, as shown in Figure 6b (Zeng et al., 2015). The underlying reaction mechanism of the nanoreactor is represented in Figure 6c. The high porosity and open pore network of the frameworks enable fast reactant/product molecules diffusion. Through π-π interaction, the organic linker of the MOFs takes 4-CP. The large pore cavity offers PMS access to the active Co_3O_4 catalytic sites, thus generating $SO_4^{\bullet-}$ radicals. The high concentration of this radical and 4-CP in a confined microenvironment offers a driving force that facilitates 4-CP degradation (Zeng et al., 2015). Recently, Li's research group demonstrated the structure-performance relationship

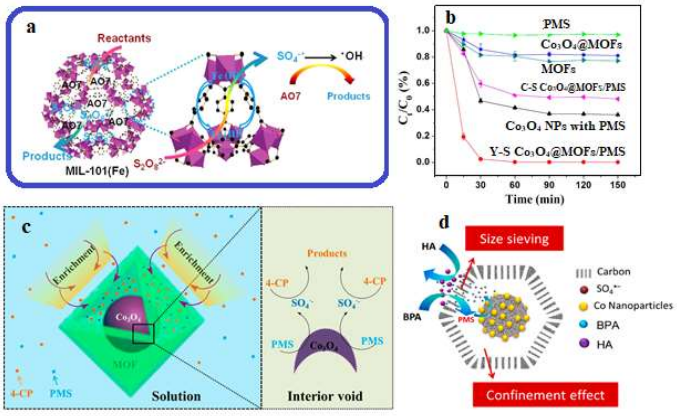

Figure 6. (a) Mechanism for the adsorptive removal of AO7 by MIL-101(Fe). Adapted with permission from Appl. Surf. Sci., 2016, 369, 130–136. (b) Removal performance of 4-CP under different conditions, (c) The plausible 4-CP degradation mechanism in the yolk-shell Co_3O_4@ MOFs nanoreactor. Permission taken from Environ. Sci. Technol., 2015, 49, 2350–2357. (d) The mechanisms of BPA degradation on the yolk-shell Co/C nanoreactors. Permission taken from Environ. Sci. Technol. 2020, 54, 10289–10300.

https://doi.org/10.1201/9781003118749

between designed yolk-shell Co/C nanoreactors (YSCCNs), prepared through pyrolysis and the selective removal of bisphenol A (BPA) in the presence of 10 mg/L humic acid (HA) (Zhang et al., 2020). YSCCNs recorded an enhanced degradation rate of BPA, which is 23.1 % and 45.4 % higher than that of hollow and solid ZIF-67 derived Co/C nanoparticles (HCCNs and SCCNs), respectively. The improved activity can be due to the cooperative effects from size exclusion in the shell layer and confinement effect in the core-shell of the nanoreactor, as illustrated in Figure 12.6d (Zhang et al., 2020).

5.2. Photocatalysis

Advanced oxidation processes for water purification include Fenton processes (Fe(II)/H_2O_2), ozonation (O_3), electrochemical oxidation, UV, or solar radiation in the presence of photocatalysts, among others (Deng & Zhao, 2015). Heterogeneous photocatalysts accelerate the photochemical reaction under irradiation and the excited electrons migrate into the conduction band (CB) while the holes remain in the valence band (VB). The photoexcited carriers facilitate the degradation of organic compounds and the treatment of hazardous metal ions by the in-situ generation of reactive oxygen species (ROS), including hydroxyl radicals (•OH) (Figure 7a) (Ahmed & Haider, 2018).

Recently, MOF-based materials have attracted attention for water treatment through photocatalysis (as shown in Figure 7b) due to their unique properties of MOFs (Wang et al., 2012; Mon et al., 2018; Wang & Astruc, 2019). Many MOFs have been reported as efficient photocatalysts for dye degradation such as MB, MO, RhB, rhodamine 6G (R6G), AO7, congo red (CR), eriochrome black T (EBT), malachite green (MG) etc. under UV and visible-light irradiation and often in presence of an additional oxidant (for example, H_2O_2 or PS) (Jiang et al., 2018; Kaur et al., 2018; Dong et al., 2019). For example, Natarajan and co-workers reported three different MOFs, [Co_2 (4,40-bpy)](4,40-obb)2, [Ni_2(4,40-bpy)$_2$], 4,40-obb)$_2$. H_2O, and [Zn_2(4,40-bpy)](4,40-obb)$_2$ having band gap values of 3.11, 3.89 and 4.02 eV, respectively, which demonstrated significant photocatalytic degradation of organic dyes, such as orange G (OG), remazol brilliant blue R (RBBR), RhB, and MB (Mahata et al., 2006) through an activated complex involving M^{2+}(Figure 12.7c–f). The fast degradation demonstrated that MOF catalysts are active in the decomposition of dyes under light irradiation. Further, a series of MOFs, such as Zn(5-aminoisophthalic acid)•H_2O, [Co_3(BPT)$_2$(DMF)(bpp)]. DMF, GR/MIL-53(Fe), Ti(IV)-based MOF structure (NTU-9), Cd(II)-imidazole MOFs, ZIF-8, and others, demonstrated high activity for dye degradation under solar light (Gao et al., 2014; Jing et al., 2014; Liu et al., 2014; Dias & Petit, 2015; Wang et al., 2015a; Zhao et al., 2015). In these MOFs, the ligand molecule donates an electron to the metal center, which facilitated the oxidation of organic molecules.

However, most of the MOFs are photocatalytically active under UV light due to large band gap and only a few, like MIL-53 or MIL-88A, absorb light in the visible region with low band gap. Even in this case, they usually need additional inorganic oxidants like H_2O_2, $KBrO_3$, and $(NH_4)_2S_2O_8$ to achieve satisfactory efficiency for organic pollutants degradation (Du et al., 2011; Xu et al., 2014).

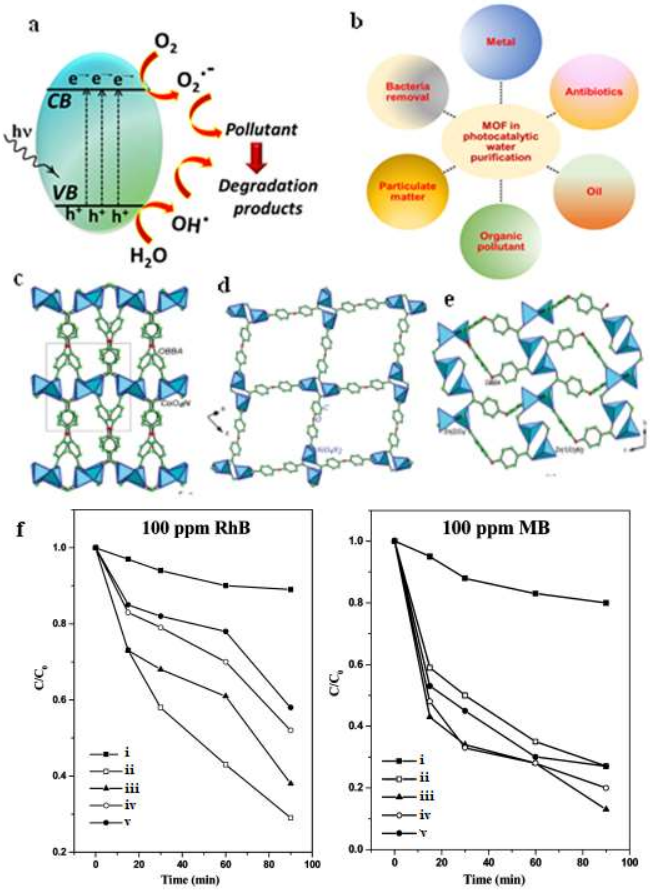

Figure.7. (a) Photocatalytic organic pollutant degradation mechanism, (b) possible application of MOF in photocatalytic water treatment. Layer structure formed by the connectivity between the (c) Co^{2+} and OBA anions, (d) Ni^{2+} ions and OBA anions, (e) Zn^{2+} and OBA. (f) Degradation profiles of two representative dyes with an initial concentration of 100 mg/L without catalyst (i), in presence of Degussa P-25 (ii), compound [Co_2(4,40-bpy)](4,40-obb)$_2$(iii), [Ni_2(4,40-bpy)$_2$](4,40-obb)$_2$•H_2O(iv), and [Zn_2(4,40-bpy)](4,40-obb)$_2$,(v). Permission taken from J. Phys. Chem. B, 2006, 110, 13759–13768.

Basically, ZIFs consist of divalent cations such as Zn2+ or Co^{2+} that are tetrahedrally coordinated to imidazolate ligands, with proven high thermal and chemical stability, were also tested for photocatalytic dye removal. Zhang and co-workers studied ZIF-67and Cu/ZIF-67 (band gaps 1.98 and 1.95 eV, respectively) for the photocatalytic degradation of MO under visible-light illumination (Yang et al., 2012). Additionally, a novel Cu-MOFs prepared with a mixture of O, N-donor

https://doi.org/10.1201/9781003118749

ligands (imidazole- and pyridine- based ligands) was able to degrade about 70–80% of dye molecules, such as MO, RhB, and MB, under the irradiation of visible light in less than 4 h, as reported by Qiao et al. (2017).

Furthermore, the fabrication of MOF-based heterostructures with other photoactive materials (metal nanoparticles, metal oxides decoration, or free-metal semiconductors) is a promising approach to improve the photocatalytic activity of MOFs due to the strong interaction of the components in intimate contact that create abundant reactive sites, thereby enhancing visible light absorption, improving charge separation with suitable energy band gap, and promoting stability (Gautam et al., 2020; Wang et al., 2020).

For example, Luo et al. (2017) developed a hierarchical TiO_2NS@MIL-100(Fe) heterostructure through the combination of MIL-100(Fe) into TiO2 nanosheets, which demonstrated enhanced photocatalytic decomposition of MB under the irradiation of visible light. Porous MOFs with high surface area facilitate efficient electron transfer and charge separation at the interface.

Due to the narrow band gap of bismuth-based semiconductors, MOFs are widely combined with compounds like Bi_2WO_6, Bi_2MoO_6, and BiOBr for the removal of dyes under visible light. Wu and co-workers (Sha et al., 2014) obtained Bi_2WO_6 assembled on a zirconium-based MOF, UiO-66 (Zr) and used it for the removal of RhB under visible light, which was complete after 3 h, due to a catalytic activity that strongly depended on Bi:Zr ratio. An improved version achieved the complete elimination of RhB in 15 min by using BiOBr/UiO-66(Zr) composite as photocatalysts. Its higher activity was attributed to enhanced charge separation that favored the generation of reactive radical species (Sha & Wu, 2015). A AgI/UiO-66 composite photocatalyst proved high stability when examined during repeated RhB degradation under visible light (Sha et al., 2015).

The presence of graphene can also improve the degradation of dyes using MOFs as photocatalysts. For example, MIL-53(Fe)–rGO (reduced graphene oxide) showed good efficiency for the degradation MB when using 2.5 % of rGO on MIL-53(Fe), attributed to electron transfer from MOF to graphene that suppressed electron-hole recombination (Zhang et al., 2014). An interesting heterojunction was reported, using g-C_3N_4 as a metal-free semiconductor (band gap, 2.70 eV) coupled with different MOFs to increase the dye degradation rate.

Wang et al. (2015b) fabricated a g-C_3N_4/Ti-benzenedicarboxylate (MIL-125(Ti)) heterostructured photocatalyst that showed high catalytic activity for RhB degradation. They proposed that the Ti^{3+}–Ti^{4+} intervalence electron transfer and the indirect dye photosensitization may improve photodegradation performance. Similarly, other MOFs such as MIL-100(Fe) and UiO-66 were also combined with g-C_3N_4 showing remarkable photocatalytic performance due to the electron transfer in the metal-oxo-clusters, and intimate contact at the interface of heterostructures which favors charge separation (Hong et al., 2016) Very recently, a ternary nanocomposite photocatalyst (MOF-Nd/GO/Fe3O4) exhibited stable, and high photocatalytic performance for the degradation of MB (~95 % in 80 min) under sunlight irradiation due to fast electron migration, slow photogenerated charge recombination, and improved optical absorption (Bai et al., 2020).

Besides organic dyes, pharmaceutical products such as tetracycline (TC) can be removed through photocatalytic degradation using a BiOI/MIL-125(Ti) composite as photocatalyst (Jiang et al., 2021). It has been reported that 9 wt % BiOI/MIL-125(Ti) composite showed 80% of degradation of TC under visible-light illumination with good stability and reusability. In another study, Abazari et al. (2020) reported the photocatalytic efficiency of Zn(II)-based MOF@Ni–Ti layered double hydroxide composite for the degradation of the antibiotic sulfamethoxazole (>98 % in 45 minutes) under solar light irradiation. MIL-68(In)-NH2/graphene oxide composite displayed 93 % photodegradation efficiency of amoxicillin when irradiated with visible light (Yang et al., 2017).

MOFs can also effectively remove Pb, Hg, Cd, and Cr using adsorption and photocatalytic processes (Chen et al., 2020). For instance, MOFs and their composites have been applied photocatalytically to reduce Cr(VI) (Liang et al., 2015; Shi et al., 2015). Moreover, g-C3N4/MIL-153(Fe) composites also showed high catalytic activity for the reduction of Cr(VI) due to the inhibition of charge recombination and the presence of highly active sites at the interface (Huang et al., 2017). Similarly, rGO modified MIL-53(Fe) also demonstrated activity for the photoreduction of Cr(VI) with up to 100 % yield after 80 min under visible light attributed to the fast transfer of photogenerated electrons at the interface between both components (Liang et al., 2015). A Cr(VI) photoreduction rate of 13.3 mg Cr(VI)/$g_{catalyst}$/min was recorded with cationic Ru-UiO-dmbpy as photocatalysts under visible-light illumination (Zheng et al., 2020). Ti-benzenedicarboxylate and amino-functionalized Ti-benzenedicarboxylate showed efficient activity for Cr(VI) reduction from aqueous solution under visible light in acidic medium (Wang et al., 2015c). Recently, a core-shell structure hybrid photocatalytic material (IR-MOF3@COF-LZU1) has been tested for the removal of nitroaromatic explosives (4-nitrophenol) under visible light (Zhao et al., 2020).

Hence, MOFs can be considered a new photocatalyst with potential applications in water treatment, including organic pollutant degradation and removal of metal

https://doi.org/10.1201/9781003118749

ions. Compared to traditional photocatalysts, MOFs possess several advantages:

-High degree of crystallinity and variety of morphologies.

- Possibility of fine-tuning structures at the molecular level, with different electronic structures.

- Availability of active sites to harvest solar light more efficiently.

- High porosity and surface area.

- Facile formation of composites with semiconductors.

In spite of having superior features for photocatalysis, very limited semiconducting behavior occurs in MOFs. The low stability of many MOFs in the presence of water may also hamper their practical applications in solar catalysis for water treatment. However, a better understanding of the photocatalytic mechanisms in MOF materials and structure-function correlation is required to optimize photocatalytic activity.

5.3. Adsorption of contaminants

The ion-exchange chemistry of metal–organic frameworks is still in an early stage and most of the reported works are still proof-of-principle studies that show the suitability of MOFs as sorbents. Unlike conventional sorbents that are mainly cationic-exchange materials (Ezugwu et al., 2013), for MOFs most studies have been done in the exchange of anionic species rather than their cationic counterparts, due to the positive charge of most metal nodes of the frameworks. Nevertheless, cation-exchange MOFs can be prepared by choosing the suitable charged ligand or PSM strategies to provide the desired amount of negative charges to the framework. Compared to conventional ion-exchange materials, MOFs have some advantages, such as: tunable structural feature, high-porous surface area (offering more area/surface for host-guest interaction), and a high degree of crystallinity (Kumar et al., 2017). Accordingly, both cationic and anionic MOF adsorbents have been successfully applied for the removal of organic pollutants via ion-exchange interaction. Through ion-exchange mechanisms, selective capturing of toxic oxoanions of arsenic As(V): ($HAsO_4^{2-}$) and selenium Se(VI): (SeO_4^{2-}) with maximum adsorption capacity of 85 and 100 mg g^{-1} have been achieved using cationic MOFs material (iMOF-C) (Sharma et al., 2020).

Neutral polytopic organic ligands (1,8-diazabicyclooctan, 4,4′-bipyridine and others) together with some polycarboxylate ligands are usually employed for the synthesis of MOFs with anion-exchange characteristics. Such MOF-based materials have been used to remove toxic anionic species, like carcinogenic Cr(VI), selenium, arsenic, phosphate anions, and others.

The adsorption of arsenate from water using MIL-53(Fe) and MIL-53(Al) has been explored and adsorption in both cases was ascribed to the interaction between trivalent metal sites of the MOFs and the oxyanion (Li et al., 2014; Vu et al., 2015). By experimental and computational analysis, Jun et al. (2015) reported the effect of open metal sites of MIL-100(Fe), Figure 8a, in the adsorption of organo-arsenic compounds. In addition, the effect of different metal nodes was studied using the adsorption of p-arsanilic acid on MIL-100(Al), MIL-100(Cr) and MIL-100(Fe). Among these three analogous MIL-100 species, MIL-100(Fe) showed the highest p-arsanilic acid adsorption capacity, assigned to the facile desorption of water from the MIL-100(Fe) and the large replacement energy, higher than that of MIL-100-Cr and MIL-100-Al. Fourier-transform infrared (FTIR) analysis was used to confirm the Fe–O–As coordination motif. Other studies highlighted the binding of anionic species to metal nodes of MOFs facilitated by labile binding of water and hydroxyl ligands. It was the case Zr6 nodes of NU-1000, which, together with a large 30 Å apertures, provided fast adsorption of selenite (100 mg g^{-1}) and selenate (62 mg g^{-1}), higher than to other Zr-based MOFs (Howarth et al., 2015a). Selenium oxyanions bridged to the Zr6 node in Zr–O–Se–O–Zr with the configuration, as shown in Figure 8b.

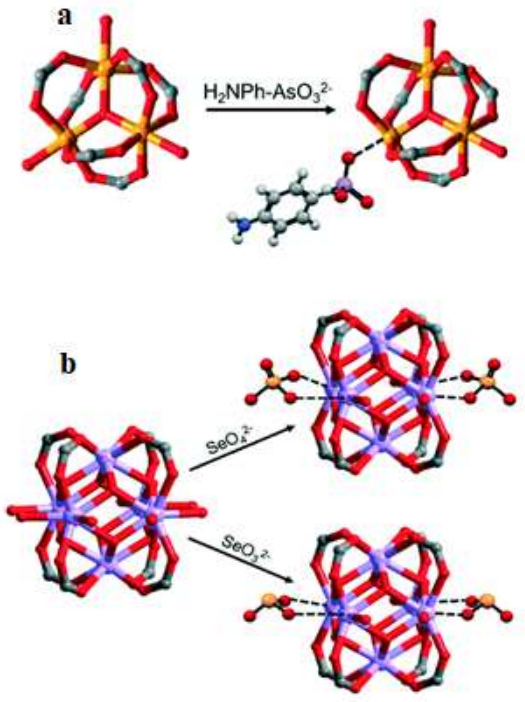

Figure 8. (a)The p-arsanilic acid adsorption mechanism on the metal cluster of MIL-100(Fe) (Jun et al., 2015), (b) Interaction of selenite and selenate on the Zr6 node of NU-1000. Permission taken from CrystEngComm, 2015, 17, 7245–7253.

UiO-66 and UiO-66-NH_2 have been applied at different temperatures for the sorption of phosphate anions (Lin et al., 2015b). For an initial concentration of ~40 mg/L, the adsorption capacity of both MOFs reached~60

https://doi.org/10.1201/9781003118749

mg/g, whereas increased capture capacity was achieved at higher temperatures: for UiO-66-NH_2, 120 and 140 mg/g of phosphate anions were removed at 40°C and 60 °C, respectively. Amine-based MOFs interact with phosphate through amine-phosphate hydrogen bonds, thus adsorbing more than UiO-66 under the same conditions.

Using MOFs for the removal of cationic species has been studied using UiO-68-P(O)$(OH)_2$ and UiO-68-P(O)$(OEt)_2$ with the uranyl cation (UO_2^{2+}) from seawater showing adsorption capacities of 188 and 217 mg g^{-1}, respectively (Carboni et al., 2013). In this case, the adsorption mechanism was attributed to the coordination between one UO_2^{2+} and the phosphorylurea groups, as shown in Figure 9.

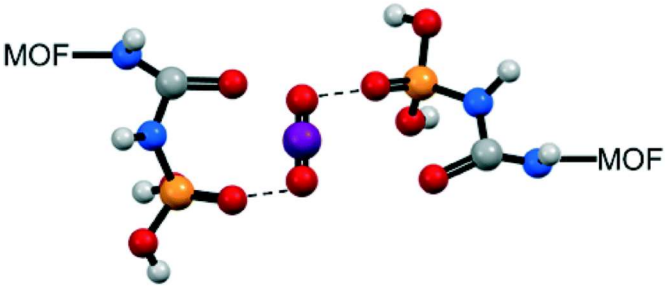

Figure 9. Interaction between the phosphorylurea functional groups and UiO-68-P(O)$(OH)_2$ for the capture of uranyl. Permission taken from CrystEngComm, 2015, 17, 7245–7253.

Other commonly available heavy metal/metalloid pollutants include mercury (Hg), lead (Pb), arsenic (As), cadmium (Cd) and chromium (Cr) (Chen et al., 2020). Even at low concentrations, heavy metal ions are highly toxic (Azimi et al., 2017).

Due to the structural diversity of MOFs, different metal ion-exchange capacities ranging from 10 to 100 mg g^{-1} can be achieved. Depending on the targeted metal ion, MOFs displayed different selectivity. The incorporation of diverse functional groups via pre-, in-situ-, or post-functionalization of the organic ligand or the metal cluster in MOFs results in physical or chemical adsorptive removal of metal ions pollutants.

Guo and co-workers employed MOF-derived inorganic materials for the adsorptive removal of Pb(II) from water (Chen et al., 2016a). They fabricated nanoporous ZnO/ZnFe2O4/C adsorbents using Fe(III)-modified MOF-5 as a precursor. The nanoporous inorganic adsorbents displayed a maximum Pb(II) adsorption capacity of 345 mg g^{-1}, and the results of the spectroscopic analysis suggested that a significant portion of Pb(II) substituted Zn(II) on the surface of the ZnO nanocrystals. Moreover, the strong magnetic behavior of Pb-containing ZnO/$ZnFe_2O_4$/C adsorbents allowed their easy separation from water using a magnet.

Although many MOFs have proved good Pb (II) adsorption capacity, most of them showed poor removal performance at low Pb(II) concentrations (Ricco et al., 2015). However, carbomethoxy-group-based MOFs (Yu et al., 2018) had been prepared through a mixed ligand synthetic approach using (pyridin-3-yl)methyl 4-(2-(4-((pyridin-3-yl)methoxy)-phenyl)diazenyl) benzoate and 2,2′-azodibenzoic acid. The as-synthesized MOF was able to quickly and completely remove trace amounts of toxic Pb(II) from water, as shown in Figure 10. At Pb(II) concentration as low as 100 mg/L, the as-prepared frameworks achieved 96 % removal efficiency, even reaching the drinking water standard (0.01 mg/L) recommended by World Health Organization (WHO). The high Pb(II) removal performance even at low concentration was attributed to the strong affinity the carbomethoxy groups, toward Pb(II). In addition, fast kinetic rate constant of 0.162 g mg^{-1} min^{-1} was recorded, higher than that for most Pb(II) adsorbents (Yu et al., 2018). Another example has been reported by Afshariazar et al. (2020), in this case, N1, N2-di(pyridine-4-yl)oxalamide) was integrated into the pores of Zn(II)-MOF, TMU-56, for the Pb(II) ions removal. TMU-56 is densely decorated with oxamide motif (-NH-CO-CO-NH-), a dual functionality promoting host-guest interaction in the framework cavities. The large pore size, together with the high densities of strong metal chelating sites explained the uptake capacity for the adsorption of Pb(II) ions (Afshariazar et al., 2020). Interestingly, the ion-exchange reaction is favored at high Pb(II) concentration, thereby resulting in a high degree of metal exchange and high removal capacity.

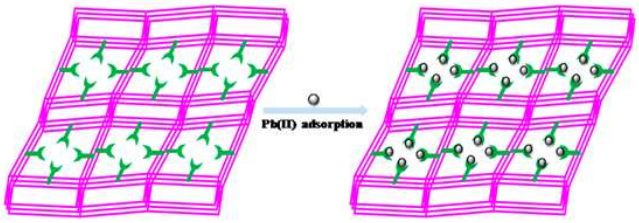

Figure 10. Carbomethoxy-functionalized MOF for Pb(II) removal. Reproduced with permission from Cryst. Growth Des. 2018, 18, 1474–1482.

Furthermore, the experimental adsorption parameters fitted well with the Langmuir isotherm, which confirmed monolayer-type adsorption (Awad et al., 2017). In the adsorption isotherm, a maximum adsorption of 1130 mg Pb/g TMU-56 was recorded (Afshariazar et al., 2020). From the XRD and IR results, the adsorption mechanism was assigned to the chelation of Pb(II) on the oxamide moiety followed by the ion-exchange reactions. This results in the replacement of some of the Zn(II)ions in the MOFs with Pb(II) ions (Afshariazar et al., 2020). Nevertheless, the oxamide motif plays the major role for the fast and high capture of Pb(II) ions from water.

Amino-decorated MOFs, MIL-101-NH_2 have demonstrated potential not only for detecting Fe^{3+}, Pb^{2+},

and Cu^{2+} but also for their adsorptive removal from aqueous solution with a capacity of 3.5, 1.1, and 0.9 m moL/g, respectively (Lv et al., 2019). In addition, other MOFs functionalized with amino groups, such as MIL-101-NH2(Cr), MIL-53-NH2(Al), MOF-5-NH2(Zn) and UiO-66-NH_2(Zr), exhibit similar sensing and capturing capacity for metal ions. Generally, MOF's fluorescence is due to the linker. Fluorescence quenching upon adsorption is based on the chemical chelation between the surface NH_2 groups and the metal ions, thereby inducing host-guest electron transfer as shown in Scheme 3 (Lv et al., 2019). Thus, the fluorescence amino-functionalized MIL-101(Fe) had a good sensing performance for detecting metal ions.

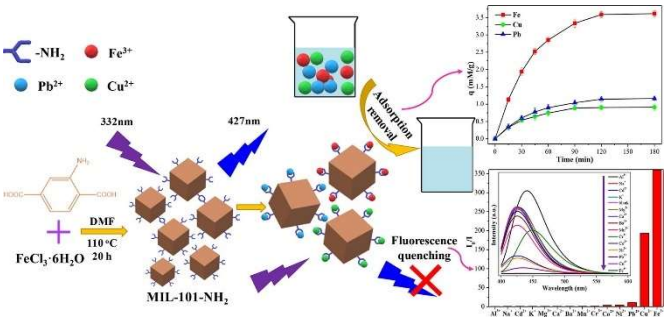

Scheme 3. Illustration of the removal and detection of heavy metals by MIL-101-NH_2. Permission taken from Chem. Eng. J., 2019, 375, 122111.

Clark et al. (2019) also employed Zr-based MOFs, UiO-66 containing several defects for the adsorptive removal of perfluorooctanesulfonate (PFOS) from simulated industrial wastewater. Defective UiO-66 was also effective for perfluorobutanesulfonate (PFBS), which is the shorter-chain homologue of PFOS. Defective MOFs showed higher adsorption capacity than the non-defective frameworks (UiO-66-DF), like sample UiO-66-10 (with 10 % vol. HCl), exhibited a 300 % increase in PFOS capture capacity over UiO-66-DF. Large-pore defects within UiO-66 reported as ~16 and ~20 Å significantly promoted PFOS adsorption from an aqueous solution. The defective UiO-66 material displayed a maximum Langmuir sorption capacity (monolayer adsorption of PFOS) of 1.24 mmol/g, which is twofold higher than activated carbon, and proceeded two-orders of magnitude faster than GAC and commercially available ion-exchange resin (Clark et al., 2019). The mechanism for PFOS adsorption on the defective UiO-66, supported by zeta potential analysis, was based on the electrostatic interaction between the sulfonate headgroup and the coordinatively unsaturated (CUS) Zr^{4+} sites together with the decreasing framework hydrophobicity (which depends on structural defectiveness) (Liang et al., 2016).

Ibuprofen (IBP) and diclofenac (DCF) are among the most useful nonsteroidal anti-inflammatory drugs used worldwide. Owing to the reason that PPCPs are used in large quantities, they are easily detected in wastewater. Although PPCPs are usually biodegradable, they are found in water bodies because of their continuous input, a phenomenon referred to as pseudo-persistency (Chen et al., 2016). Bhadra et al. (2017) used porous carbons derived from MOF (PCDMs) to remove IBP and DCF from water. PCDMs were prepared by the pyrolysis of ZIF-8 at several temperatures (800 °C, 1000 °C, and 1200°C), the sample prepared at 1000 °C exhibiting the best adsorption capacity for IBF and DCF: 320 and 400 mg/g, respectively. Based on the pH effect and the zeta potential of PCDM, the proposed adsorption mechanism is H-bonding interaction, as observed in other applications, which implies H-donation from the adsorbent (mainly via the phenolic group) and H-acceptance from DCF or IBP as shown in Scheme 4 (Bhadra et al., 2017).

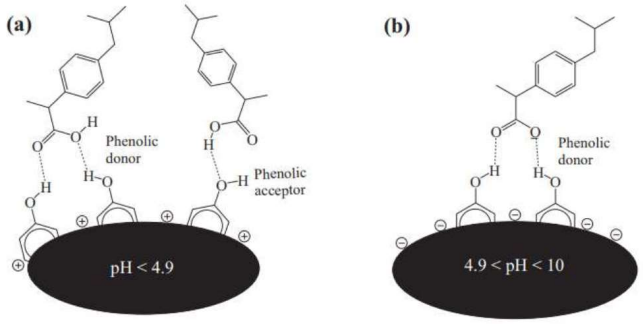

Scheme 4. Proposed adsorption mechanism of IBP on PCDM at different pH range (a) pH < 4.9 and (b) 4.9 < pH < 10. Reproduced with permission from Chem. Eng. J., 2017, 314, 50–58.

MOFs together with MOF-based materials have been successfully used for Cr(VI) adsorption with many frameworks that demonstrated outstanding adsorption capacity. Yang and co-workers reported that a cationic silver-triazolate MOF, with a formular ($[Ag_8(tz)_6](NO_3)_2 \cdot 6H_2O$) n (tz = 3,5- diphenyl-1,2,4-triazolate), displayed a fast and high Cr(VI) capture via anion exchange (Li et al., 2017). The anion-exchange behavior of 1-NO_3 followed the Hofmeister bias due to the hydrophobicity of the framework pores. During the adsorption process, the nitrates in 1-NO_3 were replaced by the Cr(VI) oxyanion. Within 15 mins, 40 % of the Cr(VI) in the aqueous solution was removed and the white powder of the silver-triazolate MOFs turned orange. At equilibrium, an adsorption capacity of 22.6 mg/g (1.35 mol mol^{-1}) was recorded. The reversibility of Cr(VI) was studied by immersing the Cr(VI)-loaded sample in an excess amount of $NaNO_3$. After 5 h, 97 % of Cr(VI) was released from 1-NO_3 (Li et al., 2017). MOFs-based magnetic polydopamine@ ZIF-8 (MP@ZIF-8) afforded Cr(VI) capture capacity of 137 mg/g (Zhu et al., 2017). The interaction was explained by the synergistic adsorption and reduction of Cr(VI) by the hybrid microsphere. The Cr(VI) adsorption-reduction mechanisms were examined by X-ray photoelectron spectroscopy (XPS), showing that during the process, the N atoms on ZIF-8 and PDA were

https://doi.org/10.1201/9781003118749

reduced, resulting in the conversion of Cr(VI) into less toxic Cr(III), further immobilized onto the MP@ZIF-8.

5.3.1. More on the mechanism of adsorption

The underlying adsorption mechanisms for metal ion pollutants removal using MOFs absorbents are normally verified by spectroscopic measurements, such as FTIR and XPS. These measurements help to evaluate the interaction between the framework materials and the metal ion. The common mechanisms for adsorptive removal of contaminants are ion exchange, coordination with the MOFs' metal nodes, and binging with the linker's functional moiety/group.

The work of Yu et al. (2018), explained Pb(II) adsorption based on its binding with the C=O unit from the carbomethoxy linker as shown in Figure 11a. The FTIR analysis of the MOFs after Pb(II) adsorption revealed a peak at 696 cm^{-1} (Figure 12.11b) ascribed to the Pb-O stretching vibration, which confirmed that Pb(II) was absorbed into the frameworks(Yu et al., 2018). In addition, new bands occurred at 798 and 1378 cm^{-1}, implying that NO_3^- is presence for charge balance (Lebrero et al., 2002). There is a red shift (1713 to 1706 cm^{-1}) attributed to the C-O vibration, confirming the coordination between the Pb(II) and the O atom of C=O unit (Zhao et al., 2015). Furthermore, the interaction of Pb(II) with the MOFs was unveiled by the XPS measurement before and after adsorption. The occurrence of Pb 4f, Pb 4d, and Pb 4p peaks undoubtedly confirmed that Pb(II) was attached to the framework after adsorption. Furthermore, the XPS spectrum of Pb 4fshowedPb 4f5/2 (143.1 eV) and Pb 4f7/2(138.2 eV) peaks. Comparing the Pb 4f XPS spectrum for the Pb(II)-loaded MOFs and purified $Pb(NO_3)_2$, it was unveiled that Pb 4f5/2 and Pb 4f7/2peaks for the MOFs appeared at 143.1 and 138.2 eV, while that of $Pb(NO_3)_2$ was observed at 144.5 eV and 139.6 eV, respectively. The lower shift in the binding energy (BE) by1.4 eV for the Pb(II)-loaded MOFs was attributed to the strong interaction between Pb(II) and the MOFs material. Overall, the two spectroscopic analyses confirmed that the carbomethoxy moiety played an important role in Pb(II) adsorption coupled with the fact that methoxy and diazene (free-standing groups) did not participate in the Pb(II) adsorption process. Therefore, the underlying adsorption mechanism follows that the of C=O unit from the carbomethoxy groups preferentially complex with the Pb(II) without the participation of the N atoms of the diazene group, since O is more electronegative than N (Yu et al., 2018)

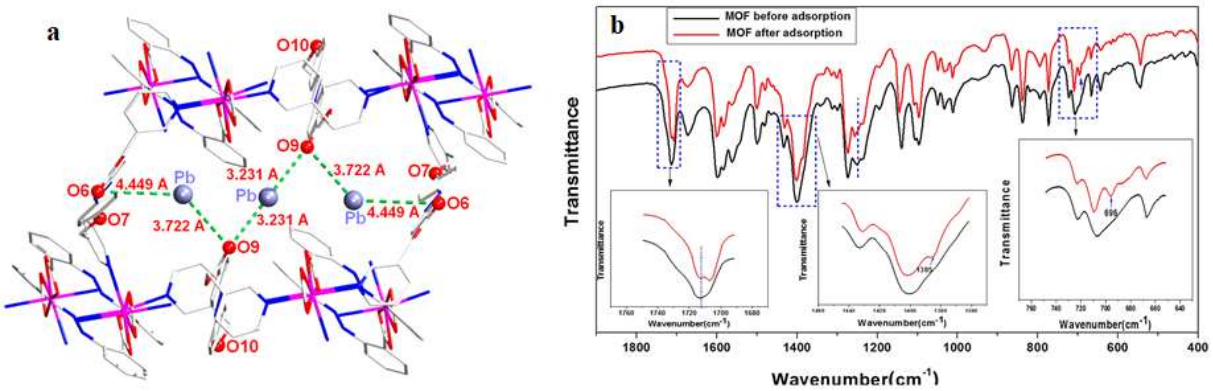

Figure 11. (a) The interaction between Pb(II) and MOF, and (b) the FT-IR spectra before and after. Reproduced with permission from Cryst. Growth Des. 2018, 18, 1474–1482

5.4. MOF-based membranes

Membrane technology in wastewater treatment has become an important solution for several processes in cosmetics, dairy, drugs, and chemical industries. Suitable approaches for the design of MOF-based membranes are important to achieve accurate and rapid wastewater purification. Numerous techniques have been established for the preparation of MOF-based membranes, such as the solvothermal method (Chen et al., 2020; Xixi et al, 2020) phase inversion, (Lee et al., 2015) (porous) mixed matrix, (Katayama et al., 2019; Liu et al., 2018) thin film nanocomposite (TFN) (Zhang et al., 2019) and electrodeposition method (Hou et al., 2019). The properties and performance of membranes can be enhanced by incorporating fillers like titanium oxide and zeolites. It is the case of mixed matrix membranes (MMM) that can be prepared using MOFs grown on a given substrate or applied as fillers to construct MOFs-mixed matrix membranes (MOF-MMMs).

For rational selection of MOFs for MMMs, the stability, dispersibility and hydrophilicity or hydrophobicity of the frameworks are crucial. Consequently, the features for ideal MOF-MMMs include highly efficient separation ability, satisfactory component stability, long-term operation capacity and, possibly, environmentally friendly preparation (Huang et al., 2017). Unlike the rigid nature of traditional inorganic frameworks, the organic linkers in novel MOFs facilitate the interactions with the polymer materials, thereby promoting good compatibility. Normally, the obtained MOF-MMMs exhibit better

permeability and selectivity than the pristine membranes (Huang et al., 2017). The most common MOFs applied for MMMs are UiO-66 (Qian et al., 2019), green MOFs (F300, C300 and A100) (Lee et al., 2014), ZIFs (Wei et al., 2020) and MIL-type MOFs (Knebel et al., 2016). Specifically, four synthesis routes are applicable for the fabrication of MOF-MMMs: layer-by-layer (LBL), in situ growth, blending technique, and gelatin-assisted seed growth. These techniques are aimed to improve MOF-based membranes for enhanced separation, like membrane distillation, adsorption desalination and capacitive deionization (Jun et al., 2020).

By modifying the pore size and chemical properties, the application of MOF-based membranes for gas separation can be extended for wastewater treatment. Zhu et al. (2016) used simulation and experimental studies to demonstrate the efficiency of polycrystalline ZIF membranes for desalination favored by the small pore size of the framework, between the size of hydrate ions and water molecules (Zhu et al., 2016). However, a recent investigation unveiled that ZIF-8 membranes in aqueous solution experience continuous Zn2+ leaching, thereby delimiting its application in water purification (Zhang et al., 2015). Liu et al. (2105) first used solvothermal synthetic approach to fabricate Zr-MOF UiO-66(Zr) polycrystalline membranes with satisfactory water stability and also shown to be efficient for water desalination (Liu et al., 2015). They demonstrated good multivalent ion rejection based on the size inclusion and good permeability (0.28 L m^{-2} h^{-1} bar^{-1}, for a membrane thickness of 2.0 µm). Based on various test conducted up to 170 h, no degradation of the membranes was recorded.

Wan et al. (2017) prepared narrow pore size (about 0.52 ± 0.02 nm) amine-functionalized UiO-66, which stand in-between the size of water molecules and hydrated ion (0.26 nm) and used them for seawater desalination by pervaporation at a temperature of 75 °C, demonstrating a high ionic sieving capacity (Wan et al., 2017). In another work, it was shown that the mitigation of the ligand-missing defects in polycrystalline UiO-66(Zr)-(OH)2 MOF membranes helped to enhance the membranes' Na+ rejection rate as shown in Figure 12a-c (Wang et al., 2017). The mitigation was achieved by post-synthetic defect healing (PSDH) resulting in up to 74.9 % Na^+ rejection rate and excellent hydrothermal stability in water. Moreover, the healed membranes were highly selective.

ZIF-8 is the most used ZIF family frameworks, due to its hydrophobic pores and stable tetrahedral MN4 structure, thus making it stable and resistant to organic solvents and water. Unlike conventional desalination techniques, membrane distillation (MD), with high salt rejection, low operation cost and moderate operation temperature can be used for wastewater treatment. A thin film composite (TFC) membrane containing thin ZIF-8/chitosan layer plated on the surface of polyvinylidene fluoride (PVDF) membrane was prepared for water desalination (Kebria et al., 2019). The ZIF-8/chitosan layer formation resulted in a high increase in the liquid entry pressure of water for the TFC membrane. In addition, the output of the air gap membrane distillation (AGMD) tests showed that the TFC with ZIF-8)/chitosan layer increased the permeate water flux with NaCl rejection > 99.5 %. The TFC composite also showed good antifouling capacity and stability, which was attributed to the good compatibility between ZIF-8 and chitosan (Kebria et al., 2019). TFN membranes with ZIF-8 are known to display improved reverse osmosis (RO) performance due to its high specific surface area and intrinsic microporosity (Lee et al., 2019). The effect of particle size of ZIF-8 on the RO desalination performance of a polyamide thin-film nanocomposite membrane was evaluated by Lee et al. (2019). ZIF-8 coating on the polysulfone support preceding the interfacial polymerization was strongly influenced by the particle size of the frameworks (Lee et al., 2019). It was observed that ZIF-8 with small-average size showed higher surface coverage.

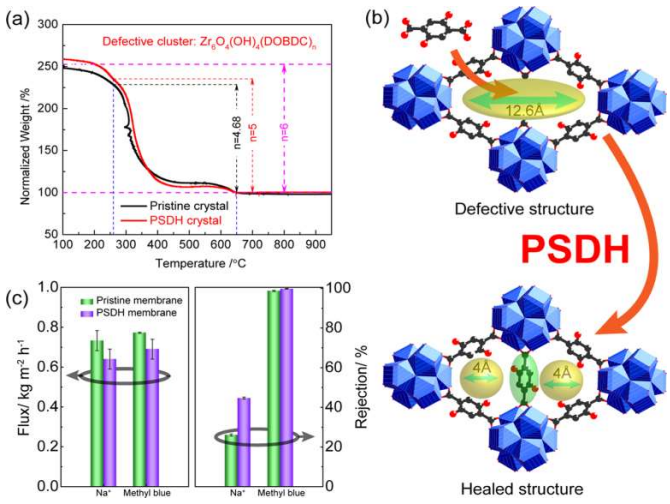

Figure 12. (a) TGA curve of UiO-66(Zr)-$(OH)_2$ frameworks before and after post-synthetic defect healing; (b) illustrating PSDH by relinking one DOBDC ligand and two adjacent $Zr_6O_4(OH)_4$ nodes and (c) The membrane's separation performance before and after PSDH. Permission taken from ACS Appl. Mater. Interfaces, 2017, 9, 37848-37855.

MOF-5-incorporated polymeric membranes of PVDF, cellulose acetate (CA) and polyethersulfone (PES) were fabricated by phase inversion method and applied for the adsorption of Co(II) and Cu(II) ions from wastewater (Gnanasekaran et al., 2019). The incorporation of MOF-5 significantly increased the hydrophilicity and rejection of both metal ions by the polymeric membranes. A high rejection efficiency was obtained for Co(II) in CA/MOF-5 and PES/MOF-5 (Gnanasekaran et al., 2019). Both the permeability flux and the rejection of PES/MOF-5, PVDF/MOF-5 and CA/MOF-5 membranes are higher compared to those recorded for the neat polymeric materials.

https://doi.org/10.1201/9781003118749

MMMs with ultrahigh MOF loading and good flexibility have been produced in a large scale. High-performance adsorption membrane was prepared by thermally induced phase separation-hot pressing (TIPS-HoP) with MOFs loadings up to 86 wt % (Wang et al., 2019). The MOF-MMMs displayed 99% rejection of organic dyes due to the adsorption on porous MOFs with a high-water flux of 125.7 L m^{-2} h^{-1} bar^{-1} under crossflow filtration mode. Interestingly, the MOF-MMMs have strong chemical and thermal robustness together with interesting mechanical strength. During the fabrication process, the MOFs were dispersed and suspended in the melt of high-density polyethylene (HDPE), ultrahigh-molecular weight polyethylene (UHMWPE) and paraffin at a 200 °C. This was followed by roll to-roll hot pressing to produce the MOF-MMMs.

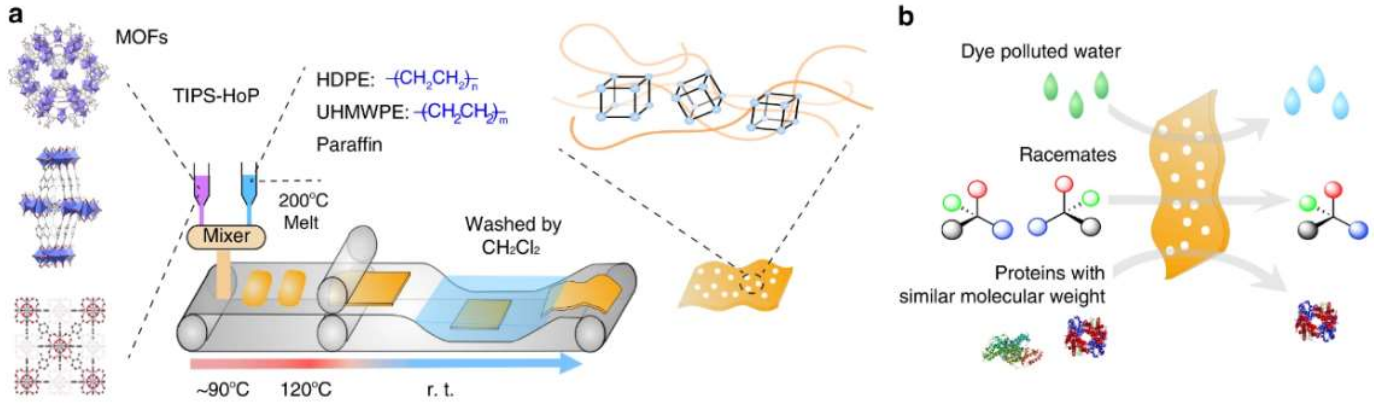

Figure 13. (a) Schematic representation for applying the TIPS-HoP technique for the fabrication of MOF PE MMMs and (b) racemates, dye and protein separations by the as-prepared MOF PE MMMs material. Reproduced with permission from Nat. Commun., 2019, 10, 1-9.

The TIPS-HoP synthetic procedure for the fabrication of MOF PE MMMs and its application for separation are illustrated in Figure 13a and b respectively. In addition, porous matrix membrane that was fabricated with MOFs as template exhibited improved porosity and enhanced separation performance (Lee et al., 2014).

6. Conclusion and prospects

Further developments in treatment of wastewater may strongly depend on advances of functional materials. The various interesting features of MOFs, such as large surface area and pore volume, high crystallinity, availability of active sites, and easy structural tunability make them attractive to create materials with the potential to outperform traditional ones. Furthermore, they can be suitably and easily tailored to obtain new functionalities by post-synthetic modifications. Therefore, they are promising materials that can be applied in the field of water purification.

As such, MOFs/MOF-derived materials have been applied in SR-AOPs. The organic ligands and the metal nodes can be modulated to enhance the activation capacity of the frameworks. Moreover, their performance can be further improved by structural/morphological optimization and fabrication of MOF composites.

As well, MOFs can be used as photocatalyst for water purification. However, most MOFs have large band gap, thus they are photo-catalytically active for the degradation of organic pollutants and pharmaceutical products under the irradiation of UV light, whereas only few with non-functionalized ligands are visible light responsive, such as MIL-53 or MIL-88A. To even achieve satisfactory performance, they usually need additional inorganic oxidants like KBrO3, and (NH4)2S2O8. The photocatalytic activities of MOFs could be also improved by preparing MOF-based heterostructures with other photoactive materials, thereby enhancing the charge separation and light absorption.

The adsorptive removal of metals/metalloid (Hg, As, Pb, Cr, and Cd) and organic pollutants from water using MOFs and MOF-derived materials have also been extensively studied, showing good performance. The functionalization of their ligand or the metal cluster, may result in an improvement of the physical or chemical adsorption. The common mechanisms for the removal of contaminants are coordination with the metal nodes of the MOFs, ion exchange and binging with the linker's functional moiety/group.

The organic ligands facilitate the interactions of the framework with polymer materials, thereby promoting good compatibility, which is very important to develop MOF based membranes. For the judicious selection of MOFs as filler for MMMs, the stability, dispersibility and hydrophilicity/hydrophobicity of the frameworks are important. UiO-66, ZIFs, green MOFs and MIL-type MOFs are commonly applied. The prepared MOF-MMMs usually have better selectivity and permeability compared to the pristine membranes.

Metal/carbon hybrids, carbon materials and metal oxides fabricated from MOFs have also showcased

https://doi.org/10.1201/9781003118749

good performance in the removal of pollutants from water.

Even though significant advances have been done for the application of MOFs in water treatment, for the commercial application of MOFs and MOF-derived materials, some aspects need to be improved, such as the synthetic conditions (high temperature and long duration in solvothermal synthesis). In addition, the stability of the frameworks in water should be enhanced. More developments are needed both by material scientists and chemists to overcome some technical issues and increase the basic knowledge of MOFs regarding structure, properties, and functional capabilities. The development of low-cost synthesis is another improvement required for their use in high-volume water treatment processes.

References

Abazari, R., Morsali, A., Dubal, D.P. 2020. An advanced composite with ultrafast photocatalytic performance for the degradation of antibiotics by natural sunlight without oxidizing the source over TMU-5@ Ni–Ti LDH: mechanistic insight and toxicity assessment. *Inorg. Chem. Front.*7: 2287-2304.

Abednatanzi, S., Derakhshandeh, P.G., Depauw, H., Coudert, F.-X., Vrielinck, H., Van Der Voort, P., Leus, K.J. 2019. Mixed-metal metal–organic frameworks. *Chem. Soc. Rev.* 48(9): 2535-2565.

Afshariazar, F., Morsali, A., Wang, J., Junk, P.C.J. 2020. Highest and Fastest Removal Rate of PbII Ions through Rational Functionalized Decoration of a Metal–Organic Framework Cavity. *Chem. Eur. J. 26*(6): 1355-1362.

Ahmed, M.M., Barbati, S., Doumenq, P., Chiron, S.J. 2012. Sulfate radical anion oxidation of diclofenac and sulfamethoxazole for water decontamination.*Chem. Eng. J.* 197: 440-447.

Ahmed, S.N., Haider, W. 2018. Heterogeneous photocatalysis and its potential applications in water and wastewater treatment: a review. *Nanotechnology* 29(34): 342001.

Ahsan, M.A., Jabbari, V., El-Gendy, A.A., Curry, M.L., Noveron, J.C. 2019. Ultrafast catalytic reduction of environmental pollutants in water via MOF-derived magnetic Ni and Cu nanoparticles encapsulated in porous carbon. *Appl. Surf. Sci.*497: 143608.

Awad, F.S., Abou-Zeid, K.M., El-Maaty, W.M.A., El-Wakil, A.M., El-Shall, M.S.J. 2017. Efficient removal of heavy metals from polluted water with high selectivity for mercury(II) by 2-imino-4-thiobiuret–partially reduced graphene oxide (IT-PRGO). *ACS Appl. Mater. Interfaces 9*(39): 34230-34242.

Azimi, A., Azari, A., Rezakazemi, M., Ansarpour, M.J. 2017. Removal of heavy metals from industrial wastewaters: a review. *ChemBioEng Rev. 4*(1): 37-59.

Bai, Y., Zhang, S., Feng, S., Zhu, M., Ma, S.J. 2020. The first ternary Nd-MOF/GO/Fe_3O_4 nanocomposite exhibiting excellent photocatalytic performance for dye degradation. *Dalton Trans.* 49: 10745-10754.

Batten, S. R., Champness, N.R., Chen, X.-M., Garcia-Martinez, J., Kitagawa, S., Öhrström, L., O'Keeffe, M., Suh, M. P., Reedijk, J. 2013. Terminology of metal–organic frameworks and coordination polymers (IUPAC Recommendations 2013). *Pure Appl. Chem. 85*(8): 1715-1724.

Bedia, J., Muelas-Ramos, V., Peñas-Garzón, M., Gómez-Avilés, A., Rodríguez, J.J., Belver, C.J. 2019. A review on the synthesis and characterization of metal organic frameworks for photocatalytic water purification. *Catalysts 9*(1): 52.

Bhadra, B.N., Ahmed, I., Kim, S., Jhung, S.H.J. 2017. Adsorptive removal of ibuprofen and diclofenac from water using metal-organic framework-derived porous carbon. *Chem. Eng. J.*314: 50-58.

Boretti, A., Rosa, L. 2019. Reassessing the projections of the world water development report. *NPJ Clean Water*. 2.1: 1-6.

Cao, W., Liu, Y., Xu, F., Li, J., Li, D., Du, G., Chen, N.J. 2019. In Situ Electrochemical Synthesis of Rod-Like Ni-MOFs as Battery-Type Electrode for High Performance Hybrid Supercapacitor. *J. Electrochem. Soc.167*(5): 050503.

Carboni, M., Abney, C.W., Liu, S., Lin, W. 2013. Highly porous and stable metal–organic frameworks for uranium extraction. *Chem. Sci.* 4.6: 2396-2402.

Chen, C., Feng, H., Deng, Y.J. 2019. Re-evaluation of sulfate radical based–advanced oxidation processes (SR-AOPs) for treatment of raw municipal landfill leachate. *Water Res.* 153: 100-107.

Chen, C., Feng, X., Zhu, Q., Dong, R., Yang, R., Cheng, Y., He, C. J. 2019. Microwave-assisted rapid synthesis of well-shaped MOF-74 (Ni) for CO_2 efficient capture. *Inorg. Chem. 58*(4): 2717-2728.

Chen, D., Shen, W., Wu, S., Chen, C., Luo, X., Guo, L. J. 2016. Ion exchange induced removal of Pb (II) by MOF-derived magnetic inorganic sorbents. *Nanoscale 8*(13): 7172-7179.

Chen, D., Zhao, J., Zhang, P., Dai, S.J. 2019. Mechanochemical synthesis of metal–organic frameworks. *Polyhedron162*: 59-64.

Chen, X., Chen, D., Li, N., Xu, Q., Li, H., He, J., Lu, J. 2020. Modified-MOF-808-Loaded Polyacrylonitrile Membrane for Highly Efficient, Simultaneous Emulsion Separation and Heavy Metal Ion Removal. *ACS Appl. Mater. Interfaces*12(35): 39227-39235.

Chen, Y., Bai, X., Ye, Z.J. 2020. Recent Progress in Heavy Metal Ion Decontamination Based on Metal–Organic Frameworks. *Nanomaterials* 10(8): 1481.

Chen, Y., Vymazal, J., Březinová, T., Koželuh, M., Kule, L., Huang, J., Chen, Z.J. 2016. Occurrence, removal and environmental risk assessment of pharmaceuticals and personal care products in rural wastewater treatment wetlands. *Sci. Total Environ.* 566: 1660-1669.

Clark, C.A., Heck, K.N., Powell, C.D., Wong, M.S. 2019. Highly defective UiO-66 materials for the adsorptive removal of perfluorooctanesulfonate. *ACS Sustain. Chem. Eng 7*(7): 6619-6628.

Cong, J., Lei, F., Zhao, T., Liu, H., Wang, J., Lu, M., Li, Y., Xu, H., Gao, J. 2017. Two Co-zeolite imidazolate frameworks with different topologies for degradation of organic dyes via peroxymonosulfate activation. *J. Solid State Chem.*256: 10-13.

Cook, T.R., Zheng, Y.-R., Stang, P.J. 2013. Metal–organic frameworks and self-assembled supramolecular coordination complexes: comparing and contrasting the design, synthesis, and functionality of metal–organic materials. *Chem. Rev. 113*(1): 734-777.

https://doi.org/10.1201/9781003118749

Deng, Y., Zhao, R.J. 2015. Advanced oxidation processes (AOPs) in wastewater treatment. *Curr. Pollut. Rep. 1*(3): 167-176.

Dias, E.M., Petit, C.J. 2015. Towards the use of metal–organic frameworks for water reuse: a review of the recent advances in the field of organic pollutants removal and degradation and the next steps in the field. *J. Mater. Chem. A 3*(45): 22484-22506.

Dong, J.-P., Shi, Z.-Z., Li, B., Wang, L.-Y. J. 2019. Synthesis of a novel 2D zinc (II) metal–organic framework for photocatalytic degradation of organic dyes in water. *Dalton Trans. 48*(47): 17626-17632.

Du, J.-J., Yuan, Y.-P., Sun, J.-X., Peng, F.-M., Jiang, X., Qiu, L.-G., Xie, A.-J., Shen, Y.-H., Zhu, J.-F.J. 2011. New photocatalysts based on MIL-53 metal–organic frameworks for the decolorization of methylene blue dye. *J. Hazard. Mater.*190: 945-951.

Du, X., Zhou, M. J. 2020. Strategies to enhance catalytic performance of metal-organic frameworks in sulfate radical-based advanced oxidation processes for organic pollutants removal. *Chem. Eng. J.*126346.

Ezugwu, C.I., Asraf, M.A., Li, X., Liu, S., Kao, C.-M., Zhuiykov, S., Verpoort, F. 2018. Cationic nickel metal-organic frameworks for adsorption of negatively charged dye molecules. *Data Brief 18*: 1952-1961.

Ezugwu, C.I., Kabir, N.A., Yusubov, M., Verpoort, F. 2016. Metal–organic frameworks containing N-heterocyclic carbenes and their precursors. *Coord. Chem. Rev 307*: 188-210.

Ezugwu, C.I., Ujam, O.T., Ukoha, P.O., Ukwueze, N.N. 2013. Complex Formation and Extraction Studies of N, N′-Bis (salicylidene)-3, 5-diaminobenzoic Acid on Hg (II) and Ag (I). *Chem. Sci. Trans. 2*: 1118-1125.

Ezugwu, C. I., Zhang, S., Li, S., Shi, S., Li, C., Verpoort, F., Yu, J., Liu, S. 2019. Efficient transformative HCHO capture by defective NH_2-UiO-66 (Zr) at room temperature. *Environ. Sci.: Nano 6*(10): 2931-2936.

Farha, O.K., Eryazici, I., Jeong, N.C., Hauser, B. G., Wilmer, C.E., Sarjeant, A.A., Snurr, R.Q., Nguyen, S.T., Yazaydin, O., Hupp, J.T. 2012. Metal–organic framework materials with ultrahigh surface areas: is the sky the limit? *J. Am. Chem. Soc. 134*(36), 15016-15021.

Furman, O.S., Teel, A.L., Watts, R.J.J. 2010. Mechanism of base activation of persulfate.*Environ. Sci. Technol. 44*(16): 6423-6428.

Furukawa, H., Ko, N., Go, Y.B., Aratani, N., Choi, S. B., Choi, E.,Yazaydin, A.O., Snurr, R.Q., O'Keeffe, M., Kim, J., Yaghi, O.M. 2010. Ultrahigh porosity in metal-organic frameworks. *Science, 329*(5990): 424-428.

Gao, J., Miao, J., Li, P.-Z., Teng, W. Y., Yang, L., Zhao, Y., Liu, B., Zhang, Q. 2014. A p-type Ti (IV)-based metal–organic framework with visible-light photo-response. *Chem. Commun. 50*(29): 3786-3788.

Gao, Y., Li, S., Li, Y., Yao, L., Zhang, H. J. 2017. Accelerated photocatalytic degradation of organic pollutant over metal-organic framework MIL-53(Fe) under visible LED light mediated by persulfate. *Appl. Catal. B Environ. 202*: 165-174.

Gautam, S., Agrawal, H., Thakur, M., Akbari, A., Sharda, H., Kaur, R., Amini, M. J. 2020. Metal oxides and metal organic frameworks for the photocatalytic degradation: A review.*J. Environ. Chem. Eng.8*(3), 103726.

George, C., Rassy, H.E., Chovelon, J.M.J. 2001. Reactivity of selected volatile organic compounds (VOCs) toward the sulfate radical (SO_4^{-}). *Int. J. Chem. Kinet. 33*(9): 539-547.

Gnanasekaran, G., Balaguru, S., Arthanareeswaran, G., Das, D.B. 2019. Removal of hazardous material from wastewater by using metal organic framework (MOF) embedded polymeric membranes. *Sep. Sci. Technol.* 54(3): 434-446.

Gong, Y., Zhao, X., Zhang, H., Yang, B., Xiao, K., Guo, T., Zhang, J., Shao, H., Wang, H., Yu, G. 2018. MOF-derived nitrogen doped carbon modified g-C_3N_4 heterostructure composite with enhanced photocatalytic activity for bisphenol A degradation with peroxymonosulfate under visible light irradiation. *Appl. Catal. B Environ.* 233: 35-45.

Gropp, C., Canossa, S., Wuttke, S., Gándara, F., Li, Q., Gagliardi, L., Yaghi, O.M. 2020. Standard practices of reticular chemistry. *ACS Cent. Sci.* 6, 8: 1255–1273.

Guillerm, V., Maspoch, D. 2019. Geometry mismatch and reticular chemistry: Strategies to assemble metal–organic frameworks with non-default topologies. *J. Am. Chem. Soc.141*(42): 16517-16538.

Haldar, D., Duarah, P., Purkait, M.K. 2020. MOFs for the treatment of arsenic, fluoride and iron contaminated drinking water: A review. *Chemosphere* 126388.

Hasan, Z., Jhung, S.H. 2015. Removal of hazardous organics from water using metal-organic frameworks (MOFs): plausible mechanisms for selective adsorptions. *J. Hazard. Mater.*283: 329-339.

Hasan, Z., Khan, N.A., Jhung, S. H. 2020. Adsorptive purification of organic contaminants of emerging concern from water with metal–organic frameworks. In Contaminants of Emerging Concern in Water and Wastewater. *Butterworth-Heinemann* 47-92.

Hong, J., Chen, C., Bedoya, F.E., Kelsall, G.H., O'Hare, D., Petit, C. 2016. Carbon nitride nanosheet/metal–organic framework nanocomposites with synergistic photocatalytic activities. *Catal. Sci. Technol.6*(13): 5042-5051.

Hou, J., Hong, X., Zhou, S., Wei, Y., Wang, H. 2019. Solvent-free route for metal–organic framework membranes growth aiming for efficient gas separation. *AIChE J. 65*(2): 712-722.

Howarth, A.J., Katz, M.J., Wang, T.C., Platero-Prats, A.E., Chapman, K.W., Hupp, J.T., Farha, O.K. 2015. High efficiency adsorption and removal of selenate and selenite from water using metal–organic frameworks. *J. Am. Chem. Soc. 137*(23): 7488-7494.

Howarth, A.J., Liu, Y., Hupp, J.T., Farha, O.K. 2015. Metal–organic frameworks for applications in remediation of oxyanion/cation-contaminated water. *CrystEngComm 17*(38): 7245-7253.

Hu, P., Long, M. 2016. Cobalt-catalyzed sulfate radical-based advanced oxidation: a review on heterogeneous catalysts and applications. *Appl. Catal. B Environ.* 181: 103-117.

Hu, P., Su, H., Chen, Z., Yu, C., Li, Q., Zhou, B., Alvarez, P. J.J., Long, M. 2017. Selective degradation of organic pollutants using an efficient metal-free catalyst derived from carbonized polypyrrole via peroxymonosulfate activation. *Environ. Sci. Technol. 51*(19): 11288-11296.

Huang, W., Liu, N., Zhang, X., Wu, M., Tang, L .2017. Metal organic framework g-C_3N_4/MIL-53(Fe) heterojunctions with enhanced photocatalytic activity for Cr(VI) reduction under visible light. *Appl. Surf. Sci.*425: 107-116.

https://doi.org/10.1201/9781003118749

Ismail, L., Ferronato, C., Fine, L., Jaber, F., Chovelon, J.-M. 2017. Elimination of sulfaclozine from water with SO_4^{-} radicals: evaluation of different persulfate activationmethods. *Appl. Catal. B Environ. 201*: 573-581.

Jiang, D., Chen, M., Wang, H., Zeng, G., Huang, D., Cheng, M., Liu, Y., Xue, W., Wang, Z. 2019. The application of different typological and structural MOFs-based materials for the dyes adsorption. *Coord. Chem. Rev. 380*: 471-483.

Jiang, D., Xu, P., Wang, H., Zeng, G., Huang, D., Chen, M., Lai, C., Wan, J.,Xue, W. 2018. Strategies to improve metal organic frameworks photocatalyst's performance for degradation of organic pollutants. *Coord. Chem. Rev.*376: 449-466.

Jiang, W., Li, Z., Liu, C., Wang, D., Yan, G., Liu, B., Che, G. 2021. Enhanced visible-light-induced photocatalytic degradation of tetracycline using BiOI/MIL-125 (Ti) composite photocatalyst. *J. Alloys Compd.*854: 157166.

Jin, A.-P., Chen, Z.-W., Wang, M.-S., Guo, G.-C. 2019. [Zn (OOCH) 2 (4, 4′-bipyridine)]$_n$: A metal-organic-framework (MOF) with x-ray-induced photochromic behaviour at room temperature. *Dyes Pigm. 163*: 656-659.

Jing, H.-P., Wang, C.-C., Zhang, Y.-W., Wang, P., Li, 2014. Photocatalytic degradation of methylene blue in ZIF-8. *RSC Adv. 4*(97): 54454-54462.

Joharian, M., Morsali, A. 2019. Ultrasound-assisted synthesis of two new fluorinated metal-organic frameworks (F-MOFs) with the high surface area to improve the catalytic activity. *J. Solid State Chem.* 270: 135-146.

Joseph, L., Jun, B.-M., Jang, M., Park, C.M., Muñoz-Senmache, J.C., Hernández-Maldonado, A.J., Heyden, A., Yu, M., Yoon, Y. 2019. Removal of contaminants of emerging concern by metal-organic framework nanoadsorbents: A review. *Chem. Eng. J.* 369:928-946.

Jun, B.-M., Al-Hamadani, Y.A., Son, A., Park, C.M., Jang, M., Jang, A., Kim, N.C., Yoon, Y. 2020. Applications of metal-organic framework based membranes in water purification: A review. *Sep. Purif. Technol.* 247: 116947.

Jun, J. W., Tong, M., Jung, B. K., Hasan, Z., Zhong, C., Jhung, S.H. 2015. Effect of central metal ions of analogous metal–organic frameworks on adsorption of organoarsenic compounds from water: plausible mechanism of adsorption and water purification. *Chem. Eur. J.* 21.1: 347-354.

Kalmutzki, M.J., Hanikel, N., Yaghi, O.M. 2018. Secondary building units as the turning point in the development of the reticular chemistry of MOFs. *Sci. Adv. 4*(10): eaat9180.

Katayama, Y., Bentz, K.C., Cohen, S.M. 2019. Defect-free MOF-based mixed-matrix membranes obtained by corona cross-linking. *ACS Appl. Mater. Interfaces 11*(13): 13029-13037.

Kaur, H., Venkateswarulu, M., Kumar, S., Krishnan, V., Koner, R.R. 2018. A metal–organic framework based multifunctional catalytic platform for organic transformation and environmental remediation. *Dalton Trans. 47*(5): 1488-1497.

Kebria, M.R.S., Rahimpour, A., Bakeri, G., Abedini, R. 2019. Experimental and theoretical investigation of thin ZIF-8/chitosan coated layer on air gap membrane distillation performance of PVDF membrane. *Desalination* 450: 21-32.

Khan, N.A., Jhung, S.H. 2017. Adsorptive removal and separation of chemicals with metal-organic frameworks: Contribution of π-complexation. *J. Hazard. Mater. 325*: 198-213.

Knebel, A., Friebe, S., Bigall, N.C., Benzaqui, M., Serre, C., Caro, J. 2016. Comparative study of MIL-96 (Al) as continuous metal–organic frameworks layer and mixed-matrix membrane. *ACS Appl. Mater. Interfaces 8*(11): 7536-7544.

Kondo, M., Yoshitomi, T., Matsuzaka, H., Kitagawa, S., Seki, K. 1997. Three-dimensional framework with Channeling cavities for small molecules: {[M2 (4, 4′-bpy) 3 $(NO_3)_4$]· xH2O}$_n$ (M Co, Ni, Zn). *Angew. Chem. Int. Ed.* 36(16): 1725-1727.

Kumar, P., Pournara, A., Kim, K.-H., Bansal, V., Rapti, S., Manos, M.J. 2017. Metal-organic frameworks: challenges and opportunities for ion-exchange/sorption applications. *Prog. Mater. Sci.* 86: 25-74.

Langmi, H.W., Ren, J., Musyoka, N.M. 2016. Metal–organic frameworks for hydrogen storage. In Compendium of Hydrogen Energy. *Woodhead Publishing* 163-188.

Lebrero, M.C.G., Bikiel, D.E., Elola, M.D., Estrin, D.O.A., Roitberg, A.E. 2002. Solvent-induced symmetry breaking of nitrate ion in aqueous clusters: A quantum-classical simulation study. *J. Chem. Phys. 117*(6): 2718-2725.

Lee, J.-Y., She, Q., Huo, F., Tang, C.Y. 2015. Metal–organic framework-based porous matrix membranes for improving mass transfer in forward osmosis membranes. *J. Membr. Sci.* 492: 392-399.

Lee, J.-Y., Tang, C.Y., Huo, F. 2014. Fabrication of porous matrix membrane (PMM) using metal-organic framework as green template for water treatment. *Sci. Rep.* 4: 3740.

Lee, K.E., Morad, N., Teng, T.T., Poh, B.T. 2012. Development, characterization and the application of hybrid materials in coagulation/flocculation of wastewater: A review. *Chem. Eng. J.* 203: 370-386.

Lee, T.H., Oh, J.Y., Hong, S.P., Lee, J.M., Roh, S.M., Kim, S.H., Park, H.B. 2019. ZIF-8 particle size effects on reverse osmosis performance of polyamide thin-film nanocomposite membranes: Importance of particle deposition. *J. Membr. Sci.* 570: 23-33.

Li, H., Eddaoudi, M., O'Keeffe, M., Yaghi, O.M. 1999. Design and synthesis of an exceptionally stable and highly porous metal-organic framework. *Nature, 402*(6759): 276-279.

Li, J., Wang, H., Yuan, X., Zhang, J., Chew, J.W. 2020. Metal-organic framework membranes for wastewater treatment and water regeneration. *Coord. Chem. Rev.* 404: 213116.

Li, J., Wu, Y.-n., Li, Z., Zhu, M., Li, F. 2014. Characteristics of arsenate removal from water by metal-organic frameworks (MOFs). *Water Sci. Technol.* 70(8): 1391-1397.

Li, L.-L., Feng, X.-Q., Han, R.-P., Zang, S.-Q., Yang, G. 2017. Cr (VI) removal via anion exchange on a silver-triazolate MOF. *J. Hazard. Mater.* 321: 622-628.

Li, W., Shi, J., Zhao, Y., Huo, Q., Sun, Y., Wu, Y., Tian, Y., Jiang, Z. 2020. Superhydrophobic Metal–Organic Framework Nanocoating Induced by Metal-Phenolic Networks for Oily Water Treatment. *ACS Sustainable Chem. Eng.* 8(4): 1831-1839.

Li, X., Guo, W., Liu, Z., Wang, R., Liu, H. 2016. Fe-based MOFs for efficient adsorption and degradation of acid

orange 7 in aqueous solution via persulfate activation. *Appl. Surf. Sci.* 369: 130-136.
Liang, R., Jing, F., Shen, L., Qin, N., Wu, L. 2015. MIL-53(Fe) as a highly efficient bifunctional photocatalyst for the simultaneous reduction of Cr(VI) and oxidation of dyes. *J. Hazard. Mater., 287*, 364-372.
Liang, R., Shen, L., Jing, F., Qin, N., Wu, L. 2015. Preparation of MIL-53(Fe)-Reduced Graphene Oxide Nanocomposites by a Simple Self-Assembly Strategy for Increasing Interfacial Contact: Efficient Visible-Light Photocatalysts. *ACS Appl. Mater. Interfaces 7*(18): 9507-9515.
Liang, W., Coghlan, C.J., Ragon, F., Rubio-Martinez, M., D'Alessandro, D.M., Babarao, R. 2016. Defect engineering of UiO-66 for CO_2 and H_2O uptake–a combined experimental and simulation study. *Dalton Trans.* 45(11): 4496-4500.
Lin, K.-Y.A., Chang, H.-A., Chen, R.-C. 2015. MOF-derived magnetic carbonaceous nanocomposite as a heterogeneous catalyst to activate oxone for decolorization of Rhodamine B in water. *Chemosphere 130*: 66-72.
Lin, K.-Y.A., Chen, S.-Y., Jochems, A.P. 2015. Zirconium-based metal organic frameworks: Highly selective adsorbents for removal of phosphate from water and urine.*Mater. Chem. Phys.*160:168-176.
Liu, C., Huang, X., Wang, J., Song, H., Yang, Y., Liu, Y., Li, J., Wang, L., Yu, C. 2018. Hollow mesoporous carbon nanocubes: rigid-interface-induced outward contraction of metal-organic frameworks. *Adv. Funct. Mater. 28*(6): 1705253.
Liu, F., Xiong, W., Liu, J., Cheng, Q., Cheng, G., Shi, L., Zhang, Y. 2018. Novel amino-functionalized carbon material derived from metal organic framework: a characteristic adsorbent for U (VI) removal from aqueous environment. *Colloids Surf. A Physicochem. Eng. Asp.*556: 72-80.
Liu, G., Chernikova, V., Liu, Y., Zhang, K., Belmabkhout, Y., Shekhah, O., Zhang, C., Yi, S., Eddaoudi, M., Koros, W.J. 2018. Mixed matrix formulations with MOF molecular sieving for key energy-intensive separations. *Nat. Mater.*17(3): 283-289.
Liu, L., Ding, J., Huang, C., Li, M., Hou, H., Fan, Y. 2014. Polynuclear CdII polymers: Crystal structures, topologies, and the photodegradation for organic dye contaminants. *Cryst. Growth Des.*14(6): 3035-3043.
Liu, X., Dang, R., Dong, W., Huang, X., Tang, J., Gao, H., Wang, G. 2017. A sandwich-like heterostructure of TiO_2 nanosheets with MIL-100 (Fe): a platform for efficient visible-light-driven photocatalysis. *Appl. Catal. B Environ.* 209: 506-513.
Liu, X., Demir, N. K., Wu, Z., Li, K. 2015. Highly water-stable zirconium metal–organic framework UiO-66 membranes supported on alumina hollow fibers for desalination. *J. Am. Chem. Soc.* 137(22): 6999-7002.
Luo, S., Wei, Z., Dionysiou, D.D., Spinney, R., Hu, W.-P., Chai, L., Yang, Z., Ye, T., Xiao, R. 2017. Mechanistic insight into reactivity of sulfate radical with aromatic contaminants through single-electron transfer pathway. *Chem. Eng. J.* 327: 1056-1065.
Luo, X., Mai, Z., Lei, H. 2019. A bifunctional luminescent Zn (II)-organic framework: Ionothermal synthesis, selective Fe(III) detection and cationic dye adsorption. *Inorg. Chem. Commun.* 102: 215-220.
Lv, S.-W., Liu, J.-M., Li, C.-Y., Zhao, N., Wang, Z.-H., Wang, S. 2019. A novel and universal metal-organic frameworks sensing platform for selective detection and efficient removal of heavy metal ions. *Chem. Eng. J.* 375: 122111.
Ma, X., Chai, Y., Li, P., Wang, B. 2019. Metal–Organic Framework Films and Their Potential Applications in Environmental Pollution Control. *Acc. Chem. Res.* 52(5): 1461-1470.
Ma, X., Li, Y., Huang, A. 2020. Synthesis of nano-sheets seeds for secondary growth of highly hydrogen permselective ZIF-95 membranes. *J. Membr. Sci.* 597: 117629.
Mahata, P., Madras, G., Natarajan, S. 2006. Novel photocatalysts for the decomposition of organic dyes based on metal-organic framework compounds. *J. Phys. Chem. B. 110*(28): 13759-13768.
Mário, E.D.A., Liu, C., Ezugwu, C.I., Mao, S., Jia, F., Song, S. 2020. Molybdenum disulfide/montmorillonite composite as a highly efficient adsorbent for mercury removal from wastewater. *Appl. Clay Sci.* 184: 105370.
Mason, J.A., Veenstra, M., Long, J.R. 2014. Evaluating metal–organic frameworks for natural gas storage. *Chem. Sci.* 5(1): 32-51.
Milenković, D.A., Dimić, D.S., Avdović, E.H., Amić, A.D., Marković, J.M.D., Marković, Z.S. 2020. Advanced oxidation process of coumarins by hydroxyl radical: towards the new mechanism leading to less toxic products.*Chem. Eng. J.* 124971.
Mon, M., Bruno, R., Ferrando-Soria, J., Armentano, D., Pardo, E. 2018. Metal–organic framework technologies for water remediation: towards a sustainable ecosystem.*J. Mater. Chem. A*6(12): 4912-4947.
Mousavi, B., Chaemchuen, S., Ezugwu, C.I., Yuan, Y., Verpoort, F. 2018. The effect of synthesis procedure on the catalytic performance of isostructural ZIF-8.*Appl. Organomet. Chem. 32*(2), e4062.
Mukherjee, S., Desai, A.V., Ghosh, S.K. 2018. Potential of metal–organic frameworks for adsorptive separation of industrially and environmentally relevant liquid mixtures. *Coord. Chem. Rev* .367: 82-126.
Neppolian, B., Doronila, A., Ashokkumar, M. 2010. Sonochemical oxidation of arsenic (III) to arsenic (V) using potassium peroxydisulfate as an oxidizing agent. *Water Res.* 44(12): 3687-3695.
Olawale, M.D., Obaleye, J.A., Oladele, E.O. 2020. Solvothermal synthesis and characterization of novel [Ni (II)(Tpy)(Pydc)]. $2H_2O$ metal-organic framework as an adsorbent for the uptake of caffeine drug from aqueous solution. *New J. Chem.* 44: 18780-18791.
Qian, Q., Wu, A.X., Chi, W.S., Asinger, P.A., Lin, S., Hypsher, A., Smith, Z.P. 2019. Mixed-matrix membranes formed from imide-functionalized UiO-66-NH2 for improved interfacial compatibility. *ACS Appl. Mater. Interfaces 11*(34): 31257-31269.
Qiao, Y., Zhou, Y.-F., Guan, W.-S., Liu, L.-H., Liu, B., Che, G.-B., Liu, C.-B., Lin, X., Zhu, E.-W. 2017. Syntheses, structures, and photocatalytic properties of two new one-dimensional chain transition metal complexes with mixed N, O-donor ligands. *Inorganica Chim. Acta* 466: 291-297.
Rastogi, A., Al-Abed, S.R., Dionysiou, D.D. 2009. Sulfate radical-based ferrous–peroxymonosulfate oxidative system for PCBs degradation in aqueous and sediment systems. *Appl. Catal. B Environ.* 85(3-4): 171-179.

https://doi.org/10.1201/9781003118749

Ricco, R., Konstas, K., Styles, M.J., Richardson, J.J., Babarao, R., Suzuki, K., Scopece, P., Falcaro, P. 2015. Lead(II) uptake by aluminium based magnetic framework composites (MFCs) in water. *J. Mater. Chem. A* 3(39): 19822-19831.

Rodríguez-Narváez, O.M., Peralta-Hernández, J.M., Goonetilleke, A., Bandala, E.R. (2017). Treatment technologies for emerging contaminants in water: a review. *Chem. Eng J. 323*, 361-380.

Rout, P.R., Zhang, T. C., Bhunia, P.,Surampalli, R.Y. 2020. Treatment technologies for emerging contaminants in wastewater treatment plants: A review. *Sci. Total Environ.* 753: 141990.

Rowsell, J.L., Yaghi, O.M. 2004. Metal–organic frameworks: a new class of porous materials. *Micropo. Mesopor. Mat.* 73(1): 3-14.

Safaei, M., Foroughi, M.M., Ebrahimpoor, N., Jahani, S., Omidi, A., Khatami, M. 2019. A review on metal-organic frameworks: synthesis and applications. *Trends. Analyt. Chem.* 118: 401-425.

Salunkhe, R.R., Kaneti, Y.V., Yamauchi, Y. 2017. Metal–organic framework-derived nanoporous metal oxides toward supercapacitor applications: progress and prospects. *ACS Nano* 11(6): 5293-5308.

Sha, Z., Sun, J., Chan, H.S.O., Jaenicke, S., Wu, J. 2015. Enhanced Photocatalytic Activity of the AgI/UiO-66 (Zr) Composite for Rhodamine B Degradation under Visible-Light Irradiation. *ChemPlusChem* 80(8): 1321-1328.

Sha, Z., Sun, J., Chan, H.S.O., Jaenicke, S., Wu, J. 2014. Bismuth tungstate incorporated zirconium metal–organic framework composite with enhanced visible-light photocatalytic performance. *RSC Adv.* 4(110): 64977-64984.

Sha, Z., Wu, J. 2015. Enhanced visible-light photocatalytic performance of BiOBr/UiO-66 (Zr) composite for dye degradation with the assistance of UiO-66. *RSC Adv.* 5(49): 39592-39600.

Sharma, S., Desai, A.V., Joarder, B., Ghosh, S.K. 2020. A Water-stable ionic MOF for the selective capture of toxic oxoanions of Se(VI) and As(V) and crystallographic insight into the ion-exchange mechanism. *Angew. Chem.* 132(20): 7862-7866.

Shayegan, H., Ali, G.A., Safarifard, V. 2020. Recent progress in the removal of heavy metal ions from water using metal-organic frameworks. *ChemistrySelect* 5(1): 124-146.

Shi, L., Wang, T., Zhang, H., Chang, K., Meng, X., Liu, H., Ye, J. 2015. An amine-functionalized iron(III) metal–organic framework as efficient visible-light photocatalyst for Cr(VI) reduction. *Adv. Sci.* 2(3): 1500006.

Siegert, M., Sonawane, J. M., Ezugwu, C.I., Prasad, R. 2019. Economic assessment of nanomaterials in bio-electrical water treatment. In Advanced Research in Nanosciences for Water Technology. *Springer International Publishing AG, Cham.* 1-23.

Smolders, S., Struyf, A., Reinsch, H., Bueken, B., Rhauderwiek, T., Mintrop, L., Kurz, P., Stock, N., De Vos, D.E. 2018. A precursor method for the synthesis of new Ce(IV) MOFs with reactive tetracarboxylate linkers. *ChemComm 54*(8): 876-879.

Song, J.Y., Bhadra, B.N., Khan, N.A., Jhung, S.H. 2018. Adsorptive removal of artificial sweeteners from water using porous carbons derived from metal azolate framework-6.*Micropor. Mesopor. Mat. 260*, 1-8.

Stock, N., Biswas, S. 2012. Synthesis of metal-organic frameworks (MOFs): routes to various MOF topologies, morphologies, and composites. *Chem. Rev. 112*(2), 933-969.

Sule, R., Mishra, A.K. 2019. Synthesis of mesoporous MWCNT/HKUST-1 composite for wastewater treatment. *Appl. Sci.* 9(20): 4407.

Taheran, M., Naghdi, M., Brar, S. K., Verma, M., Surampalli, R. Y. 2018. Emerging contaminants: Here today, there tomorrow! *Environ. Nanotechnol. Monit. Manag.* 10: 122-126.

Torad, N. L., Hu, M., Ishihara, S., Sukegawa, H., Belik, A. A., Imura, M., Ariga, K., Sakka, Y., Yamauchi, Y. 2014. Direct synthesis of MOF-derived nanoporous carbon with magnetic Co nanoparticles toward efficient water treatment. *Small* 10(10): 2096-2107.

Tranchemontagne, D.J., Mendoza-Cortés, J.L., O'Keeffe, M., Yaghi, O.M. 2009. Secondary building units, nets and bonding in the chemistry of metal–organic frameworks. *Chem. Soc. Rev.* 38(5): 1257-1283.

Tzanakakis, V.A., Paranychianakis, N.V., Angelakis, A.N. 2020. Water supply and water scarcity. *Water* 12(9): 2347.

Vardhan, H., Mehta, A., Ezugwu, C.I., Verpoort, F. 2016. Self-assembled arene ruthenium metalla-assemblies. *Polyhedron 112*: 104-108.

Vu, T.A., Le, G.H., Dao, C.D., Dang, L.Q., Nguyen, K.T., Nguyen, Q.K., Dang, P.T., Tran, H.T.K., Duong, Q.T., Nguyen, T.V., Lee, G.D. 2015. Arsenic removal from aqueous solutions by adsorption using novel MIL-53 (Fe) as a highly efficient adsorbent. *RSC Adv.* 5(7): 5261-5268.

Wan, L., Zhou, C., Xu, K., Feng, B., Huang, A. 2017. Synthesis of highly stable UiO-66-NH_2 membranes with high ions rejection for seawater desalination. *Micropor. Mesopor. Mat. 252*: 207-213.

Wang, C., Kim, J., Malgras, V., Na, J., Lin, J., You, J., Zhang, M., Li, J., Yamauchi, Y. 2019. Metal–organic frameworks and their derived materials: Emerging catalysts for a sulfate radicals-based advanced oxidation process in water purification. *Small* 15(16): 1900744.

Wang, C., Liu, X., Demir, N.K., Chen, J.P., Li, K. 2016. Applications of water stable metal–organic frameworks. *Chem. Soc. Rev. 45*(18): 5107-5134.

Wang, F., Dong, C., Wang, C., Yu, Z., Guo, S., Wang, Z., Zhao, Y., Li, G. 2015. Fluorescence detection of aromatic amines and photocatalytic degradation of rhodamine B under UV light irradiation by luminescent metal–organic frameworks. *New J. Chem.* 39(6): 4437-4444.

Wang, H., Yuan, X., Wu, Y., Zeng, G., Chen, X., Leng, L., Li, H. 2015. Synthesis and applications of novel graphitic carbon nitride/metal-organic frameworks mesoporous photocatalyst for dyes removal. *Appl. Catal. B Environ.* 174: 445-454.

Wang, H., Yuan, X., Wu, Y., Zeng, G., Chen, X., Leng, L., Wu, Z., Jiang, L., Li, H. 2015. Facile synthesis of amino-functionalized titanium metal-organic frameworks and their superior visible-light photocatalytic activity for Cr(VI) reduction. *J. Hazard. Mater.* 286: 187-194.

Wang, H., Zhao, S., Liu, Y., Yao, R., Wang, X., Cao, Y., Ma, D., Zou, M., Cao, A., Feng, X., Wang, B. 2019.

https://doi.org/10.1201/9781003118749

Membrane adsorbers with ultrahigh metal-organic framework loading for high flux separations. *Nat. Commun.* 10(1): 1-9.
Wang, J.-L., Wang, C., Lin, W. 2012. Metal–organic frameworks for light harvesting and photocatalysis. *ACS Catal. 2*(12): 2630-2640.
Wang, J., Wang, S. 2018. Activation of persulfate (PS) and peroxymonosulfate (PMS) and application for the degradation of emerging contaminants. *Chem. Eng. J.* 334: 1502-1517.
Wang, Q., Astruc, D. 2019. State of the art and prospects in metal–organic framework (MOF)-based and MOF-derived nanocatalysis. *Chem. Rev.* 120(2): 1438-1511.
Wang, Q., Gao, Q., Al-Enizi, A. M., Nafady, A., Ma, S. 2020. Recent advances in MOF-based photocatalysis: environmental remediation under visible light. *Inorg. Chem. Front.* 7(2): 300-339.
Wang, X., Zhai, L., Wang, Y., Li, R., Gu, X., Yuan, Y. D., Qian, Y., Hu, Z., Zhao, D. 2017. Improving water-treatment performance of zirconium metal-organic framework membranes by postsynthetic defect healing. *ACS Appl. Mater. Interfaces 9*(43): 37848-37855.
Wei, J.-Z., Gong, F.-X., Sun, X.-J., Li, Y., Zhang, T., Zhao, X.-J., Zhang, F.-M. 2019. Rapid and low-cost electrochemical synthesis of UiO-66-NH_2 with enhanced fluorescence detection performance. *Inorg. Chem.* 58(10): 6742-6747.
Wei, W., Liu, J., Jiang, J. 2020. Atomistic simulation study of polyarylate/zeolitic-imidazolate framework mixed-matrix membranes for water desalination. *ACS Appl. Nano Mater*. 3(10): 10022–10031.
Xiao, R., Luo, Z., Wei, Z., Luo, S., Spinney, R., Yang, W., Dionysiou, D.D. 2018. Activation of peroxymonosulfate/persulfate by nanomaterials for sulfate radical-based advanced oxidation technologies. *Curr. Opin. Chem. Eng.* 19: 51-58.
Xu, S., Lv, Y., Zeng, X., Cao, D. 2017. ZIF-derived nitrogen-doped porous carbons as highly efficient adsorbents for removal of organic compounds from wastewater. *Chem. Eng. J. 323*, 502-511.
Xu, W.-T., Ma, L., Ke, F., Peng, F.-M., Xu, G.-S., Shen, Y.-H., Zhu, J.-F., Qiu, L.-G., Yuan, Y.-P.2 014. Metal–organic frameworks MIL-88A hexagonal microrods as a new photocatalyst for efficient decolorization of methylene blue dye. *Dalton Trans.* 43(9): 3792-3798.
Yaghi, O. M., Li, G., Li, H. 1995. Selective binding and removal of guests in a microporous metal–organic framework. *Nature* 378(6558): 703-706.
Yaghi, O.M., O'Keeffe, M., Ockwig, N.W., Chae, H.K., Eddaoudi, M., Kim, J. 2003. Reticular synthesis and the design of new materials. *Nature* 423(6941): 705-714.
Yang, C., You, X., Cheng, J., Zheng, H., Chen, Y. 2017. A novel visible-light-driven In-based MOF/graphene oxide composite photocatalyst with enhanced photocatalytic activity toward the degradation of amoxicillin.*Appl. Catal. B Environ.* 200: 673-680.
Yang, D., Babucci, M., Casey, W.H., Gates, B.C. 2020. The surface chemistry of metal oxide clusters: from metal–organic frameworks to minerals. *ACS Cent. Sci.* 6(9): 1523-1533.
Yang, H., He, X.-W., Wang, F., Kang, Y., Zhang, J. 2012. Doping copper into ZIF-67 for enhancing gas uptake capacity and visible-light-driven photocatalytic degradation of organic dye. *J. Mater. Chem.* 22(41): 21849-21851.
Yang, S., Wang, P., Yang, X., Shan, L., Zhang, W., Shao, X., Niu, R. 2010. Degradation efficiencies of azo dye Acid Orange 7 by the interaction of heat, UV and anions with common oxidants: persulfate, peroxymonosulfate and hydrogen peroxide. *J. Hazard. Mater.*179(1-3): 552-558.
Yu, C., Han, X., Shao, Z., Liu, L., Hou, H. 2018. High efficiency and fast removal of trace Pb (II) from aqueous solution by carbomethoxy-functionalized metal–organic framework. *Cryst. Growth Des. 18*(3): 1474-1482.
Zeng, T., Zhang, X., Wang, S., Niu, H., Cai, Y. 2015. Spatial confinement of a Co_3O_4 catalyst in hollow metal–organic frameworks as a nanoreactor for improved degradation of organic pollutants. *Environ. Sci. Technol.* 49(4): 2350-2357.
Zhang, D.-S., Zhang, Y.-Z., Gao, J., Liu, H.-L., Hu, H., Geng, L.-L., Zhang, X., Li, Y.-W. 2018. Structure modulation from unstable to stable MOFs by regulating secondary N-donor ligands. *Dalton Trans. 47*(39): 14025-14032.
Zhang, H., Liu, D., Yao, Y., Zhang, B., Lin, Y.S. 2015. Stability of ZIF-8 membranes and crystalline powders in water at room temperature. *J. Membr. Sci.* 485: 103-111.
Zhang, M., Xiao, C., Yan, X., Chen, S., Wang, C., Luo, R., Qi,. J., Sun, X., Wang, L., Li, J. 2020. Efficient removal of organic pollutants by metal–organic framework derived Co/C yolk–shell nanoreactors: size-exclusion and confinement effect. *Environ. Sci. Technol.* 54(16): 10289-10300.
Zhang, X., Zhang, Y., Wang, T., Fan, Z., Zhang, G. 2019. A thin film nanocomposite membrane with pre-immobilized UiO-66-NH_2 toward enhanced nanofiltration performance. *RSC Adv.* 9(43): 24802-24810.
Zhang, Y., Li, G., Lu, H., Lv, Q., Sun, Z. 2014. Synthesis, characterization and photocatalytic properties of MIL-53 (Fe)–graphene hybrid materials. *RSC Adv.* 4: 7594–7600.
Zhang, Y., Zhou, J., Feng, Q., Chen, X., Hu, Z. 2018. Visible light photocatalytic degradation of MB using UiO-66/g-C_3N_4 heterojunction nanocatalyst.*Chemosphere* 212: 523-532.
Zhao, J., Dong, W.-W., Wu, Y.-P., Wang, Y.-N., Wang, C., Li, D.-S., Zhang, Q.-C. 2015. Two (3, 6)-connected porous metal–organic frameworks based on linear trinuclear [$Co_3(COO)_6$] and paddlewheel dinuclear [$Cu_2(COO)_4$] SBUs: gas adsorption, photocatalytic behaviour, and magnetic properties. *J. Mater. Chem. A* 3(13): 6962-6969.
Zhao, J., Jin, B., Peng, R. 2020. New Core–Shell Hybrid Material IR-MOF3@COF-LZU1 for Highly Efficient Visible-Light Photocatalyst Degrading Nitroaromatic Explosives. *Langmuir 36*(20): 5665-5670.
Zhao, S.-N., Zhang, Y., Song, S.-Y., Zhang, H.-J. 2019. Design strategies and applications of charged metal organic frameworks. *Coord. Chem. Rev.* 398: 113007.
Zhao, Y., Song, M., Cao, Q., Sun, P., Chen, Y., Meng, F. 2020. The superoxide radicals' production via persulfate activated with $CuFe_2O_4$@ Biochar composites to promote the redox pairs cycling for efficient degradation of o-nitrochlorobenzene in soil. *J. Hazard. Mater.* 400: 122887.

https://doi.org/10.1201/9781003118749

Zheng, H.-Q., He, X.-H., Zeng, Y.-N., Qiu, W.-H., Chen, J., Cao, G.-J., Lin, R.-G., Lin, Z.-J., Chen, B. 2020. Boosting the photoreduction activity of Cr(vi) in metal–organic frameworks by photosensitiser incorporation and framework ionization. *J. Mater. Chem. A*8(33): 17219-17228.

Zhu, C., Liu, F., Ling, C., Jiang, H., Wu, H., Li, A. 2019. Growth of graphene-supported hollow cobalt sulfide nanocrystals via MOF-templated ligand exchange as surface-bound radical sinks for highly efficient bisphenol A degradation. *Appl. Catal. B Environ.* 242: 238-248.

Zhu, K., Chen, C., Xu, H., Gao, Y., Tan, X., Alsaedi, A., Hayat, T.2017. Cr(VI) reduction and immobilization by core-double-shell structured magnetic polydopamine@ zeolitic idazolate frameworks-8 microspheres. *ACS Sustainable Chem. Eng.* 5(8): 6795-6802.

Zhu, Y., Gupta, K. M., Liu, Q., Jiang, J., Caro, J., Huang, A. 2016. Synthesis and seawater desalination of molecular sieving zeolitic imidazolate framework membranes. *Desalination 385*: 75-82.

https://doi.org/10.1201/9781003118749